



1

2 Calibration guide pipe system for 3 DARKSIDE-20K TPC and Veto

4 P. Barrillon ^a, M. Carlini ^b, V. Goicoechea Casanueva ^c, F. Hubaut ^a, A. Kish ^c,
5 J. Maricic ^c, P. Pralavorio ^a, P. Skensved ^d, M. Van Uffelen ^a, I. Wingerter-Seez ^a

6 ^aCPPM, Aix-Marseille Université, CNRS/IN2P3, Marseille, France

7 ^bLaboratori Nazionali del Gran Sasso, INFN, Italy

8 ^cDepartment of Physics and Astronomy, University of Hawai'i, Honolulu, HI 96822,
9 USA

10 ^dDepartement of Physics, Engineering Physics and Astronomy, Queen's University,
11 Kingston, ON K7L 3N6, Canada

12

17th April 2023

13

Abstract

14 A detailed description of the calibration guide pipe system proposed for DARKSIDE-20K
15 is presented. It consists of two pipes running on the side of the TPC and below, to serve
16 as a radioactive source guide. Each pipe is equipped with one motor at each extremity;
17 a rope is attached to both motors and allows to transport the source from one extremity
18 to the other by slowly pulling the rope and maintaining the right tension. This allows to
19 precisely position the source. The sources are inserted and fixed to the ropes through
20 dedicated glove boxes. The two guide tubes have been implemented in the official simula-
21 tion package and this note presents a first tentative TPC calibration program for photon
22 and neutron sources. The impact of the presence of the tubes for the light collection
23 efficiency in the veto buffer and the corresponding induced ER and NR backgrounds is
24 also given. Design and hardware implementation are discussed. To address the two main
25 challenges (robustness of the calibration system against freezing of the pipe and/or a
26 source getting stuck in the pipe) two mock-ups have been built. Obtained Results and
27 future plans are given in this note.

<i>CONTENTS</i>	<i>CONTENTS</i>
28 Contents	
29 1 Introduction	3
30 2 Motivations	3
31 2.1 Generalities	3
32 2.2 Calibration requirements	4
33 2.3 Calibration system overview	6
34 3 Simulation studies	8
35 3.1 Implementation of the guide tube in g4ds	8
36 3.2 Calibration with ER sources	9
37 3.3 Calibration with NR sources	20
38 3.4 Light collection efficiency in the veto buffer	24
39 3.5 Background induced by the guide tube system	27
40 3.5.1 NR background	28
41 3.5.2 ER background	29
42 3.5.3 Neutron capture and materials activation	32
43 3.6 Neutron Veto Inefficiency	33
44 4 Hardware implementation	34
45 4.1 Components and status	34
46 4.1.1 Guide tube	34
47 4.1.2 Motors	36
48 4.1.3 Glove boxes	36
49 4.1.4 Rope	36
50 4.2 Integration in DARKSIDE-20K	38
51 4.3 Operation in DARKSIDE-20K	44
52 4.4 Mock-ups	46
53 4.4.1 General characteristics of DARKSIDE-20K calibration system . .	46
54 4.4.2 Warm mock-up at scale-one (MU_W)	46
55 4.4.3 Cryogenic mock-up for short runs (MU_CS)	47
56 4.4.4 Remaining tests at CPPM	52
57 4.4.5 Cryogenic mock-up for long runs (MU_CL)	52
58 5 Conclusions	54
59 References	55
60 A Sources	56
61 B GANTT	58
62 C Costbook and Basis of Estimate (BoE)	59
63 D Risks	63
64 E Background results for ArDM stainless steel	71

2 MOTIVATIONS

1 Introduction

We propose to design and build the guide pipe system around the DARKSIDE-20K TPC that enables the movement of radioactive sources emitting photons and/or neutrons, providing the mean to calibrate energy of electron and neutron recoils (ER and NR). The installation of the guide pipe around the TPC will take place at Gran Sasso, most probably before any cold test. The system should be fully functional for the start of the experiment which is currently foreseen to take place in 2026. In this note we first review the motivations for a guide pipe systems around the DARKSIDE-20K LAr TPC (section 2). The detector description refers to the technical design report (TDR) submitted to INFN in December 2021 [1]. In section 3 the detailed simulation study of several key points associated to the calibration guide pipe system is described and conclusions on the final system are drawn. In section 4 the evolution of the guide pipe system is presented; its design, integration, operation and the description and results of the mock ups are given. Conclusions are given in Section 5

2 Motivations

DARKSIDE-20K will be the largest TPC ever built for direct dark matter searches and a dedicated effort to calibrate its response is obviously a key element. Calibrations for both the TPC and the veto detector range from low-level calibration of detector response, such as the single-photoelectron response of individual photosensors, to high-level physics calibration like the acceptance as a function of energy for nuclear recoils. A combination of radioactive sources, a neutron generator, and light sources ensures a robust calibration plan to enable DS-20k to achieve its science goals.

2.1 Generalities

A particle slowing in the argon TPC ¹ will produce 128 nm scintillation light. There are two components to the light, a prompt (\sim ns) and a delayed ($\sim \mu\text{s}$) one and the relative amounts depends on the particle. This allows to distinguish between electron and "nuclear" type events. The dual phase technology has the main advantage to provide simultaneous access to the scintillation (S1) and to the ionisation (S2) signals, as illustrated in Figure 1 left, allowing for the complete event topology reconstruction. Two types of background, illustrated in Figure 1 right, can mimick a WIMP signal : i) neutrons for which the detector response, composed of "fast" scintillation light and low number of ionisation electrons, is called Nuclear Recoil (NR) and ii) electron/photons, for which the detector response, composed of "slow" scintillation light and high number of ionisation electrons, is called Electron Recoil (ER). The former background is irreducible and therefore neutrons should be screened and/or tagged by the veto system before they reach the TPC and the latter one is reducible using the signal pulse shape. For high enough energy recoil (> 50 keV), the latter will become negligible since the pulse shape of the signal

¹For a WIMP, the typical nuclear recoil energy is in the range 10-100 keV. Note that with a S2 only analysis, where the electron drift time information is not available, the lower range can be extended to 1 keV

2.2 Calibration requirements

enables a separation by a factor greater than 10^8 between "slow" and "fast" scintillation [2, 3].

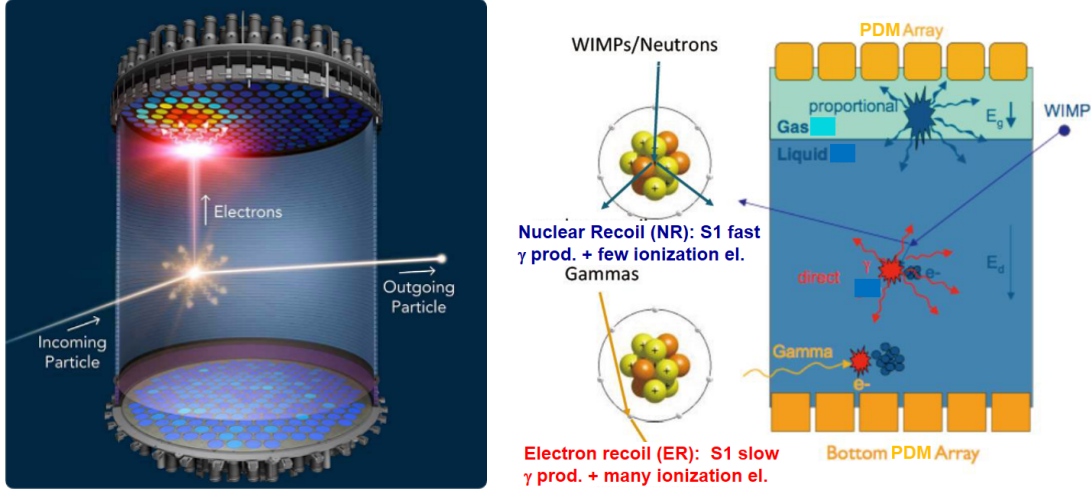


Figure 1: Left: Principle of a Dual phase TPC, with both scintillation and ionization signals. Right: The two main backgrounds for WIMP signal and their main characteristics.

2.2 Calibration requirements

Performing a search in a wide mass range requires a multi-faced calibration program, sketched in Figure 2.

The preparation of a robust physics analysis, as soon as data taking starts, includes to address a set of challenges associated to the detector calibration:

- C1 The large energy ranges to cover WIMP masses from $\simeq 1$ GeV to multi-TeV, corresponding to a range of 0.5 to 100 keV of deposited energy for NR. The range below 10 keV, can be reached by considering only the S2 signal, as demonstrated by DS-50 [4]. The corresponding range for ER background spans between 0.05 to 100 KeV. Providing means to measure the response linearity is a requirement for the calibration system.
- C2 DARKSIDE-20K will be the largest dual phase LAr TPC ever built, 1000 times larger than DS50. The uniformity and stability of the response, in space and time, of such a large the detector are essential. The calibration system coverage should be as large as technically possible, to have the ability to scan the detector response in the largest volume possible. The knowledge of the source position, with a typical precision of 1 cm, is required when calibrating low energy deposits.
- C3 The separation of NR and ER signals is an intrinsic property of LAr. By supplying both types of signals, the calibration system provides in-situ means to possibly improve the rejection.

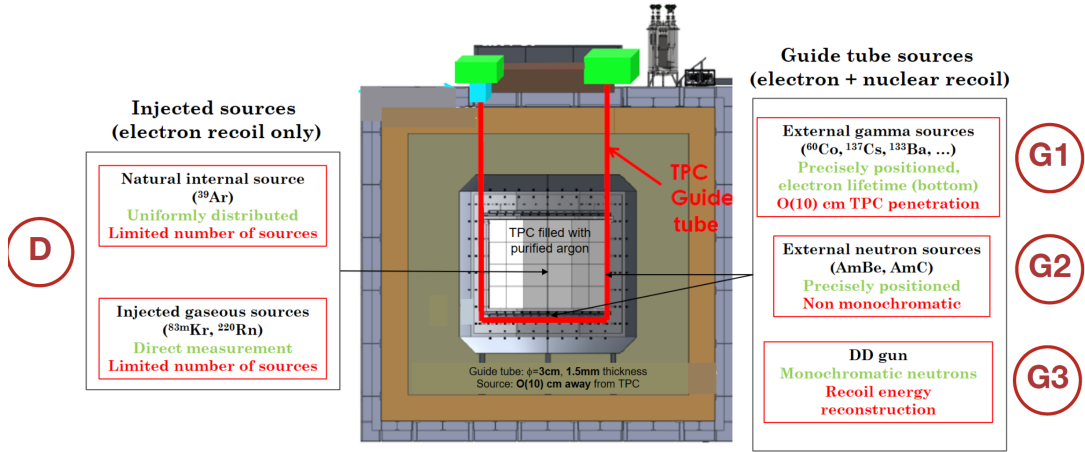


Figure 2: Sketch of the DARKSide-20K calibration program. The cryostat is represented in the center of the Figure. On the left of the cryostat, considered sources which would be injected in the liquid argon are listed; the label D refers to diffused sources in the text. On the right, considered emitters, which would be transported inside the calibration pipes, are labeled as B_n and discussed further in the text.

- 124 C4 The detector is expected to collect data for a decade, with stable performance. The
 125 calibration system gives the ability to regularly and reliably measure the detector
 126 performance and means to correct for any variation due to aging for instance.
- 127 C5 The commissioning and operation of the 200,000 SiPM requires meticulous and
 128 systematic implementation. The guide pipe calibration system will allow to check
 129 the response uniformity, the signal to noise ratio, the energy resolution.

130 To cover the energy range of interest for WIMP, 0.5 to 200 keV_{nr}, Figure 2 shows
 131 the calibration techniques in a schematic way. Two approaches are foreseen to be imple-
 132 mented: the inclusion of ^{83m}Kr and ^{220}Rn inside the TPC volume (labeled with D) and
 133 the displacement of gamma (labeled with G1) and neutron (labeled with G2 and G3)
 134 emitters in pipes around the TPC. The two approaches are complementary: the ^{83m}Kr
 135 atoms are distributed in the entire volume of the TPC, and therefore provide a mean
 136 to measure the response uniformity in the TPC; though the XY position of the emitter
 137 is not a priori known and is measured with S2. At low energy, the XY position cannot
 138 be precisely measured as the position resolution deteriorates. Emission of photons and
 139 neutrons from the guide pipe on the other hand are limited to the periphery of the TPC;
 140 the penetration of photons has a strong energy dependence.

141 It is interesting to note that the displacement of gamma sources along the vertical
 142 side of the TPC will allow to precisely measure the LAr drift time, one of the input to
 143 S1/S2 association. In addition, it could allow to measure, for instance, the thickness of
 144 the TPB layer above the photo-electronics. In DS50, a strong radial dependence of the
 145 S2 response was measured and corrected for, using events from ^{83m}Kr [5]. The origin of
 146 this non uniformity is assumed to be coming from the non-uniformity of the TPB coating,
 147 the variation of the depth of the gas-pocket or of the electric field in the gas pocket. The
 148 radial systematics is strongly related to the accuracy with which we can determine the

source position in the pipe below the TPC. A direct measurement of its thickness will reduce systematic errors associated to the reconstructed energy.

Three types of neutron emitters are considered: neutron emitters sources which produce photons, in coincidence with neutrons, which can pollute the measurement of the NR; pure gamma emitters; and pure neutrons emitters such as D-D gun. These three possibilities are discussed below.

This note concentrates on the guide pipe system which is foreseen to be installed around the TPC. Therefore laser calibration, which provides photo-sensor charge and time response is not discussed here.

2.3 Calibration system overview

Table 1 presents a summary of the challenges, the requirements and the goals, and the means of the calibration procedure in preparation for DARKSIDE-20K .

Challenge	Requirement	Calibration sources	
		ER	NR
C_1	Linearity	G_1	G_2
C_2	Uniformity	D	G_2, G_3
C_3	Pulse shape, rejection	G_1	G_2, G_3
C_4	Time stability		all
C_5	SiPM operation, S/N		all

Table 1: Summary of the challenges, requirements and goals, and means of the DARKSIDE-20K calibration system. The challenges C_n are defined in the text and the labels D or G_n refers to Figure 2.

Based on Table 1 and on practical considerations, a baseline for the calibration guide pipe system has emerged in 2020 and is now included in the 2021 TDR [1]. Figure 3 shows a detailed view of the guide pipe system. The baseline for the calibration system of the TPC consists in two U-shaped pipes of 3 cm internal diameter and 1.5 mm thickness. The preferred material for the pipes is stainless steel. The pipes will exit on the top cap of the cryostat where the glove boxes and the motor systems will be located. Section 3 presents the implementation of this calibration system in the DARKSIDE-20K simulation and propose a first calibration program. Impact of the presence of the pipes for the veto light collection efficiency and ER/NR background induced are presented in details. The hardware implementation is described in section 4.

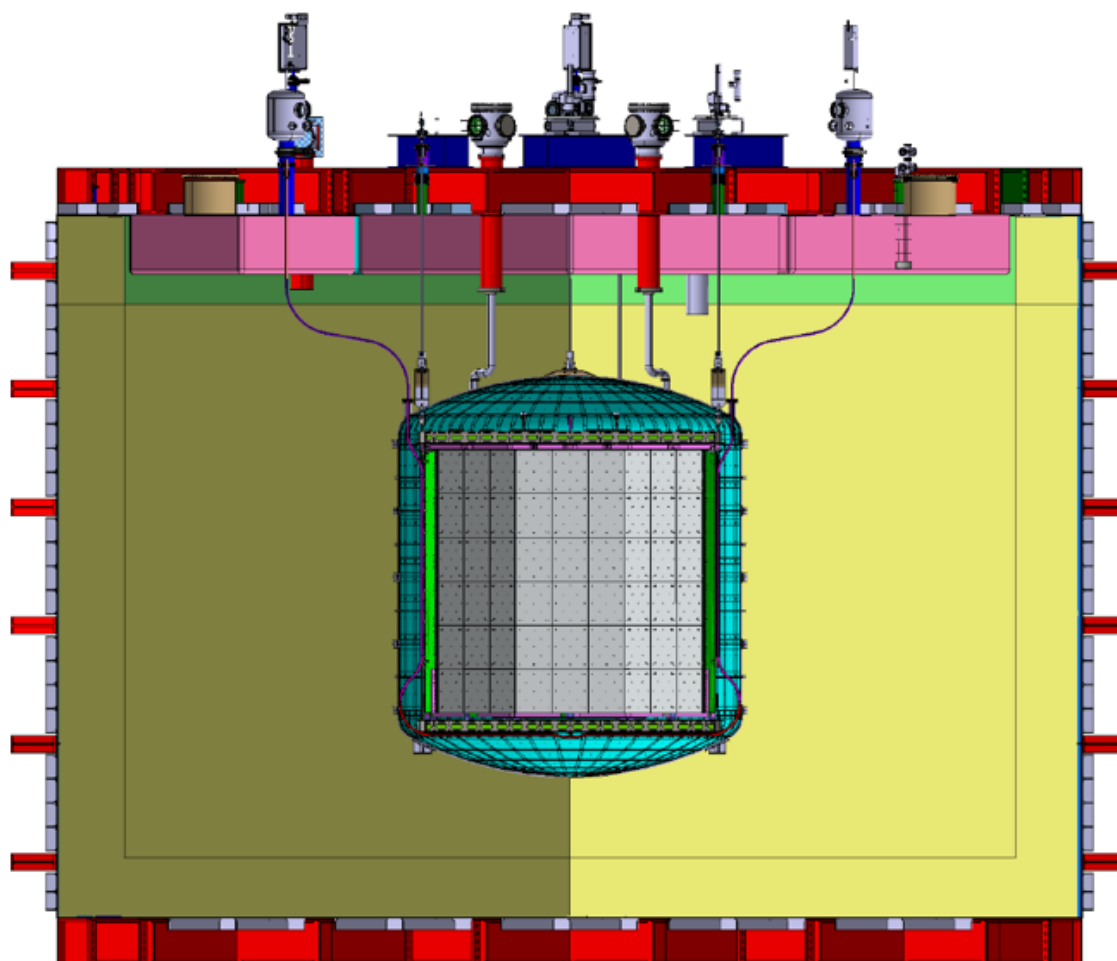


Figure 3: Schematic representation of the calibration guide pipe system. The four colours (pink, purple, magenta and red, from top to bottom) indicate the four portions of the pipes which will be welded or connected via a flange.

171 3 Simulation studies

172 3.1 Implementation of the guide tube in g4ds

173 As documented in the TDR [1], the inner detector is a vessel filled with 100t of
 174 underground liquid argon. 50t are inside an octagonal TPC and 32t are inside a cylindrical
 175 veto buffer (external part of the vessel). The side walls of the TPC will be 15 cm thick
 176 and made with acrylic doped with gadolinium. The top and bottom walls of the TPC
 177 are 10 cm thick. The SiPMs area is 10 cm thick and placed at the top and bottom of
 178 the TPC as well. Then 5 cm of acrylic (the anode (top) and the cathode (bottom)) are
 179 placed below(top)/above(bottom) the SiPMs area. Figure 4 shows how DarkSide-20k
 180 is implemented in the simulation software. The walls will permit to tag neutrons by
 181 moderating them when they cross the wall and interact with the Hydrogen of the acrylic.
 182 Then, they will be captured in the Gd, producing multiple γ -rays with energies up to 8
 183 MeV.

184 In addition to the PMMA+gadolinium walls, the veto aims at tagging neutronic back-
 185 ground before it enters the TPC and creates events while interacting with LAr. To do
 186 so, it is also equipped with SiPMs at the top and bottom and on the external parts of
 187 the GdPMMA walls, separating the TPC and the veto. LAr will produce characteristic
 188 128 nm photons, which wavelength will be shifted by Polyethylene Naphthalate (PEN)
 189 material positionned on the walls of the veto.

190

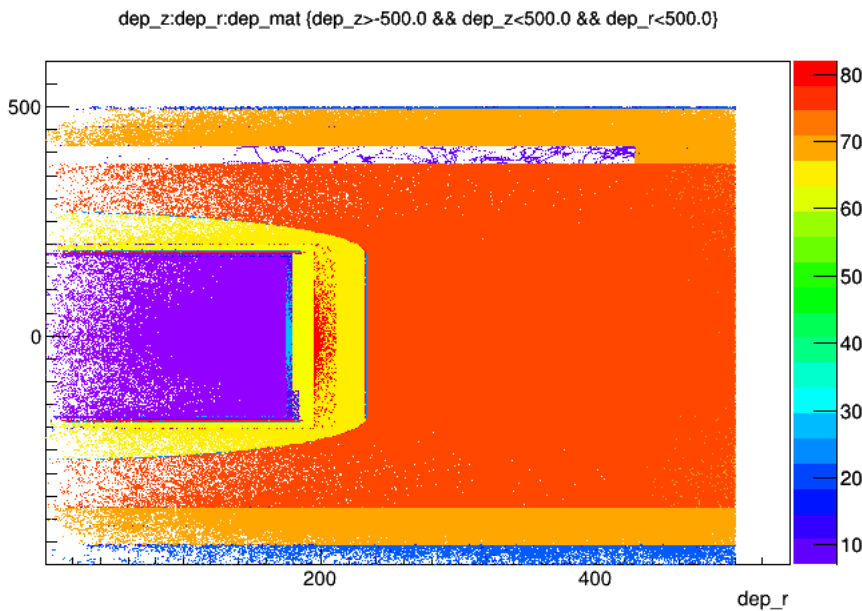


Figure 4: Overall geometry of the current design of the DarkSide-20k detector (TDR design) as it is implemented in g4ds, the simulation software created for the collaboration (based on CERN's GEANT4 software). It is an octagonal TPC (violet) with gadolinium-doped acrylic walls (light yellow, just tens of centimeters around the TPC). Around the TPC is the veto area (darker yellow). The orange colors represent the cryostat filled with atmospheric liquid argon. Axis are in cm thus the radius of the TPC is 1.9m.

3 SIMULATION STUDIES

3.2 Calibration with ER sources

The guide tubes system will be made with stainless-steel ², 3 cm of diameter ³ and 1.5 mm thick. Pipes will be placed outside the TPC, immersed in the veto buffer, 3 cm away from the walls on the side of the TPC and 1 cm under the TPC (see Figure 5-left). Figure 5 - middle and right show how the placement of the pipes is implemented inside a GEANT4 software applied to DarkSide experiment, called g4ds in the following. The two U-shaped tubes will cross under the tank without interfering thanks to a bending on the lower one.

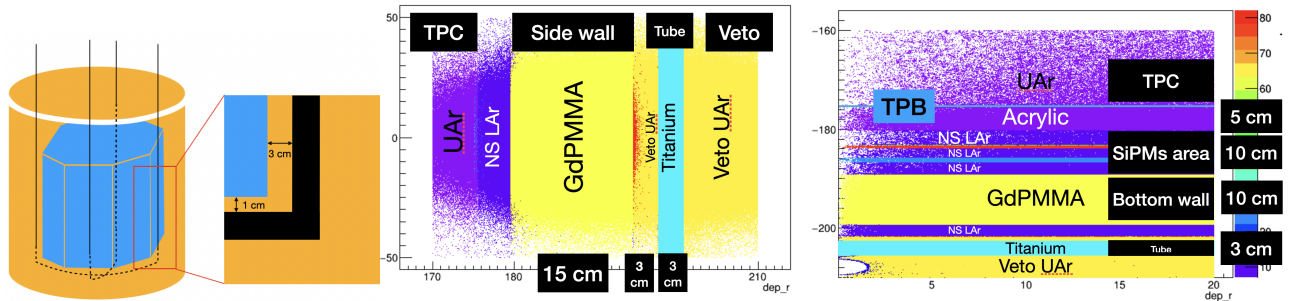


Figure 5: Left: Scheme of the settlement of the pipes around the TPC : in blue are the walls of the TPC. Around it is the beginning of the veto (the orange area). The pipes (black) are placed 3 cm away from the outer side of the TPC walls, in the veto. The lower part of the pipe will be 1 cm under the bottom of the signal reconstruction system. Middle: The side of the TPC as it is implemented in g4ds. From left to right, one can see: the TPC, the GdPMMA wall (15 cm thick), 3cm of veto buffer, 3 cm of calibration pipe, and the veto buffer. Right: The bottom of the TPC as it is implemented in g4ds. From up to down, one can see: the TPC, the cathode in PMMA (5 cm thick), the SiPM area (10 cm thick), the GdPMMA wall (10 cm thick), 1 cm of veto buffer, 3cm of calibration pipe and the veto buffer.

The energy resolution of DarkSide-20k TPC was simulated and computed with simulations of photons of energy of 10, 100, 500 and 1000 keV. The simulation points and the associated fit are shown on Figure 6. This leads to the resolution function of DS20k TPC which goes like $0.0023 + \frac{0.334}{\sqrt{E}}$, E in keV.

3.2 Calibration with ER sources

The DarkSide-20k technology allows to reach a very good energy and position reconstruction which has to be calibrated before data taking. Besides, as direct direction of WIMPs requires long data acquisition (DarkSide-20k will be run for 10 years), other calibration runs will be operated in order to check the time stability of the detector's response.

Electronic recoil (ER) signal is expected to be background for the high mass WIMP search, thus it has to be calibrated. To do so, five sources of photons (⁵⁷Co, ¹³³Ba, ²²Na,

²Titanium was foreseen in the TDR. Note that simulation results described in sections 3.2 and 3.3 were made with titanium tubes, but the impact of the change is negligible. The impact on results presented in sections 3.4 and 3.5 is discussed in these sections.

³5 cm is also an option: the impact on results presented in sections 3.4 and 3.5 is discussed in these sections.

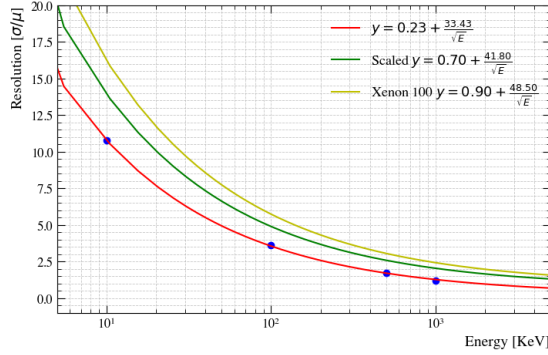


Figure 6: Energy resolution of DS20k’s TPC to photons (blue points and fit in red curve), as obtained with g4ds simulations.

²¹⁰ ^{137}Cs , ^{60}Co) whose energy span from 122 to 1173 keV (see table 2) will be used. Two
²¹¹ other sources of photons, ^{241}Am (59.5 keV) and ^{109}Cd (88 keV) were considered and
²¹² will be discussed at the end of this section. Because of the reduced penetration (O(10
²¹³ cm)), the calibration enabled by the guide tube system is non uniform, confined at the
²¹⁴ borders of the TPC. This is why another type of calibration will be achieved: calibration
²¹⁵ using short lifetime and short decay chains gaseous radioactive elements (or the relic ^{39}Ar
²¹⁶ present in the TPC) directly inserted inside LAr. These elements (such as krypton) will
²¹⁷ permit a calibration in the whole volume of the TPC, without control of the position.

²¹⁸ The most useful ER signal events are single scatter (SS) events. The events considered
²¹⁹ in this study are pure ER SS with an energy corresponding to the emitter.

Source	^{57}Co	^{133}Ba	^{22}Na	^{22}Na	^{137}Cs	^{60}Co	^{60}Co
Energy (keV)	122	356	511	1274	662	1173	1332

Table 2: Initial photons’ energy for the five sources of photons used for DarkSide-20k ER calibration.

²²⁰ In order to establish the best calibration procedure, namely choosing the sources, the
²²¹ energy spectra, estimating the duration of a calibration scan, the simulation were made
²²² with g4ds, based on GEANT4 package and the DarkSide-20k geometry as described in
²²³ the TDR.

²²⁴ This study presents simulations with sources inside the pipes, on the side and at the
²²⁵ bottom of the TPC, using 1e7 events per point. On the side, sources were at $z = 0$ (the
²²⁶ middle of the TPC side) and 4.5 cm away from the wall (tubes are placed 3 cm from the
²²⁷ wall and are 3 cm large with source at the middle). At the bottom of the TPC, sources
²²⁸ were placed at $x = y = 0$ which represents the center of the octagonal TPC face and at
²²⁹ 2.5 cm below the TPC wall (inside the tubes which are 1 cm under the bottom wall).

²³⁰ Figure 7 (resp. Figure 8) represents the rate of events per decay as a function of the
²³¹ energy deposited in the TPC for each considered source of photons positioned on the
²³² side (resp. at the bottom) of the TPC. The initial energy of photons (when they are
²³³ emitted by the radioactive sources) goes from 122 to 1372 keV. The Monte-Carlo spectra
²³⁴ are convoluted with the foreseen energy resolution of DS20k.

3 SIMULATION STUDIES

3.2 Calibration with ER sources

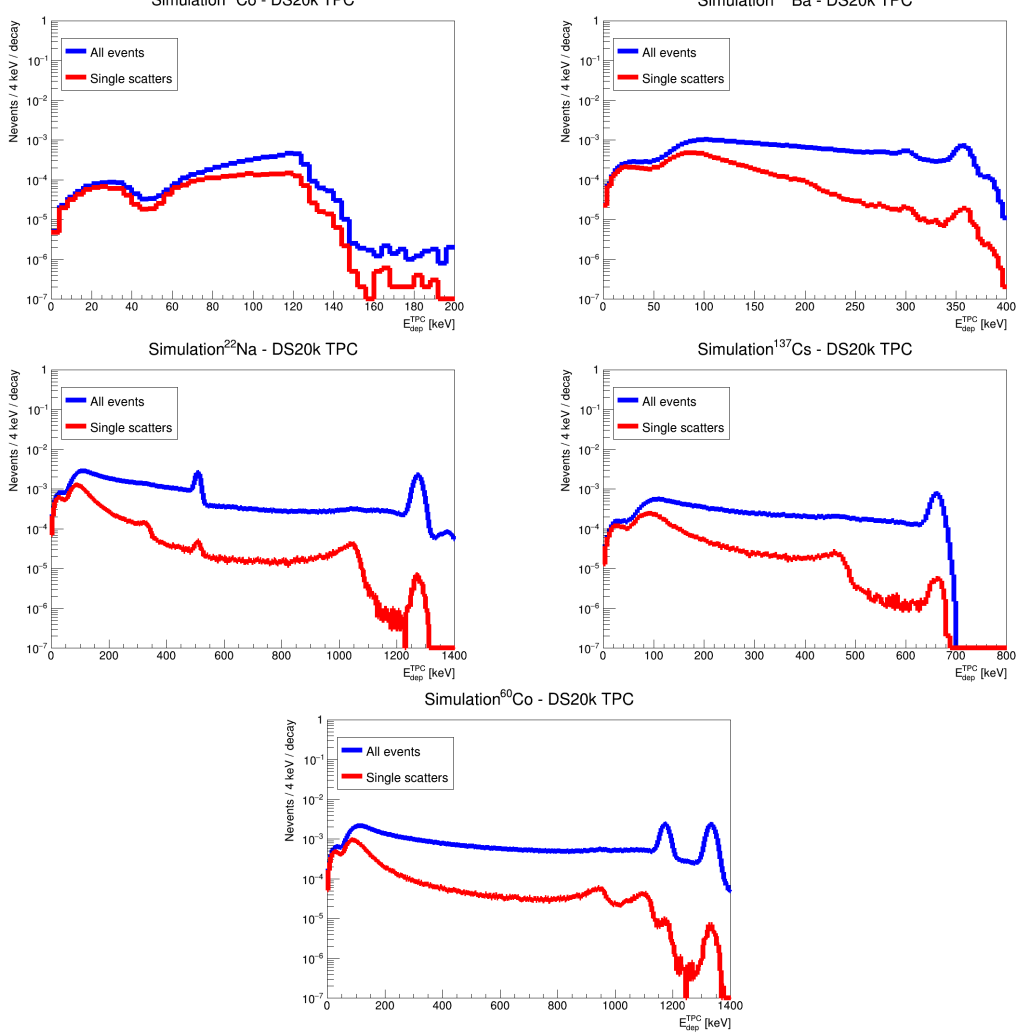


Figure 7: Rates of events per decay of the simulated source as a function of the energy deposited in the TPC, for five sources of photons. From left to right and top to bottom : ^{57}Co , ^{133}Ba , ^{22}Na , ^{137}Cs , ^{60}Co . ^{22}Na and ^{60}Co have two photoelectric peaks (see table 2). The spectra are presented for all types of events and separately for single scatters. The source was positioned on the side of the TPC. The expected energy resolution of DarkSide-20k is applied.

Source	^{57}Co	^{133}Ba	^{22}Na	^{137}Cs	^{60}Co	^{22}Na	^{60}Co
Energy (keV)	122	356	511	662	1173	1274	1332
SS - Rate - Side (events/decay)	5.7×10^{-3}	5.4×10^{-2}	2.8×10^{-1}	4.5×10^{-2}	2.8×10^{-1}	2.8×10^{-1}	2.8×10^{-1}
SS - Rate - Bot. (events/decay)	8.8×10^{-4}	2.0×10^{-2}	1.5×10^{-1}	2.2×10^{-2}	1.7×10^{-1}	1.5×10^{-1}	1.7×10^{-1}

Table 3: Rates of single scatters events for the whole energy spectra measured in the TPC per decay of the calibration source positioned inside the pipe on the side and at the bottom of the TPC.

3.2 Calibration with ER sources

3 SIMULATION STUDIES

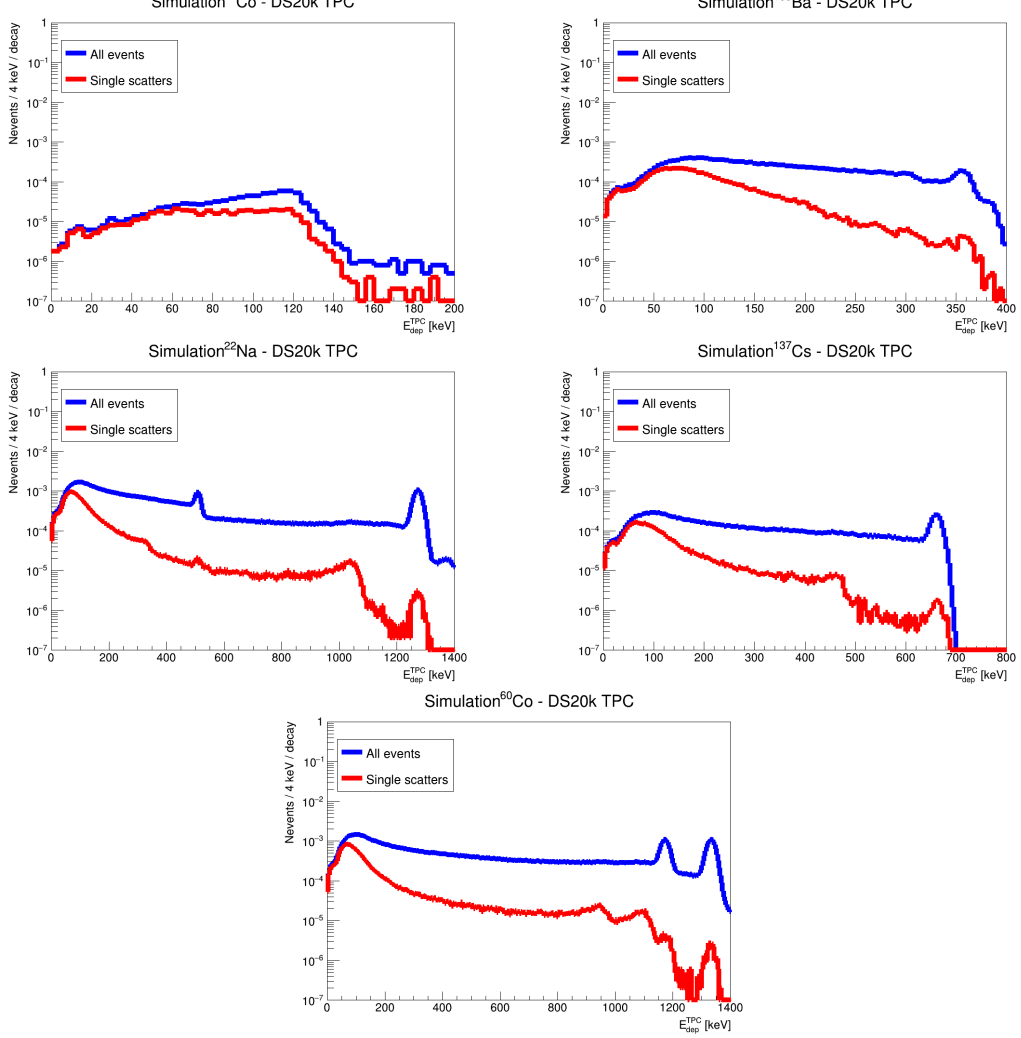


Figure 8: Rates of events per decay of the simulated source as a function of the energy deposited in the TPC, for five sources of photons. From left to right and top to bottom : ^{57}Co , ^{133}Ba , ^{22}Na , ^{137}Cs , ^{60}Co . The spectrum are presented for all types of events and separately for single scatters. The source was positioned at the bottom of the TPC. The expected energy resolution of DarkSide-20k is applied.

The table 3 presents the rates of SS computed from the energy spectra of Figures 7 and 8. The rates are rather low because of the thickness of the TPC walls: GdPMMA absorbs photons and many of them never enter the TPC. Plus, the rates on the side are two to four times higher than the ones at the bottom. Indeed, there is more passive material at the bottom of the TPC than on the side (optical planes are populated with SiPMs) and the more a photon crosses matter, the more it loses its energy.

Table 4 presents the rates of SS in the photoelectric peak of the same spectra computed between -2σ and 2σ of the peak. In average, the higher the energy, the lower the rate of SS in the peak. The photoelectric effect dominates at low energy (from 10 to ≈ 80 keV) then becomes more and more unlikely at high energy. The Compton scattering dominates at middle energy (≈ 80 keV to ≈ 5 MeV). This is why it is less and less probable to see the photoelectric peak at high energy. Thus at high energy, one could consider

3 SIMULATION STUDIES

3.2 Calibration with ER sources

Source	^{57}Co	^{133}Ba	^{22}Na	^{137}Cs	^{60}Co	^{22}Na	^{60}Co
Energy (keV)	122	356	511	662	1173	1274	1332
SS peak - Rate - Side (events/decay)	6.2×10^{-4}	1.1×10^{-4}	3.7×10^{-4}	4.0×10^{-5}	1.0×10^{-4}	5.9×10^{-5}	6.1×10^{-5}
SS peak - Rate - Bot. (events/decay)	8.2×10^{-5}	2.6×10^{-5}	1.6×10^{-4}	1.2×10^{-5}	5.2×10^{-5}	2.7×10^{-5}	2.2×10^{-5}

Table 4: Rates of single scatters events in the energy peak of the spectra measured in the TPC per decay of the calibration source positioned inside the pipe on the side and at the bottom of the TPC.

247 using the Compton edge instead (or in addition to) the photoelectric peak as it is more
 248 depictable than the peaks of energy in the SS channel. The energy of the Compton edge
 249 is well known: $E_{edge} = E_{peak} \left(1 - \frac{1}{1 + \frac{2E_{peak}}{m_ec^2}} \right)$, E_{peak} being the energy of the photoelectric
 250 peak, using it would help increasing the calibration point's liability.

251 From the ER energy spectra (Figures 7 & 8) and the tables 3 & 4 summarizing
 252 the rates of events inside the photoelectric peak for each source, one can derive a time
 253 estimate of the duration of calibration runs for one tube. The estimate is based on the
 254 following hypotheses:

- 255 1. Two hours are needed to handle the sources (to place them inside the tubes and
 256 remove them at the end of the run).
- 257 2. Data will be taken at nine positions : three on each side of the TPC and three
 258 others at the bottom of the TPC.
- 259 3. At each position, the calibration takes 1,000 gold SS events at the peak energy (so
 260 that the uncertainty $\sigma = \frac{\sqrt{N}}{N} = \frac{32}{1,000} = 3.2\%$) or 10,000 SS in the whole energy
 261 range of the spectrum.
- 262 4. The signal reconstruction system saturates at 100 Hz.
- 263 5. The activity of the sources are computed such that they saturate the signal recon-
 264 struction system. For the time being, such activities are different for the positions
 265 on the side of the TPC and at the bottom (because the rates are different in both
 266 positions). If the activity needed to saturate the reconstruction system exceeds 100
 267 kBq, it saturates at 100 kBq in order to have reasonable activities.

268 Considering first the whole energy spectra and focusing on single scatter events, the
 269 table 3 presents the rates of such events. These rates are between 3×10^{-1} and 10^{-3} .

270 Table 5 presents the results for these hypotheses, and for 10,000 events: typically five
 271 hours for each of the five sources are needed. Therefore the ER calibration should last a
 272 full day. Such a procedure would provide spectra with reasonable statistics as presented
 273 on Figures 9 & 10.

3.2 Calibration with ER sources

3 SIMULATION STUDIES

Source	^{57}Co	^{133}Ba	^{22}Na	^{137}Cs	^{60}Co
Energy (keV)	122	356	511	662	1173
Activity (side) (kBq)	18	1.9	0.36	2.2	0.36
Activity (bottom) (kBq)	100	5.0	0.67	4.6	0.6
Duration of calibration (h)	4.2	4.6	5.2	5.0	5.4

Table 5: Activity needed and time estimation for the ER calibration using 10,000 SS events for the whole energy spectra of the sources. The time needed to perform the ER calibration run in one pipe is one day straight.

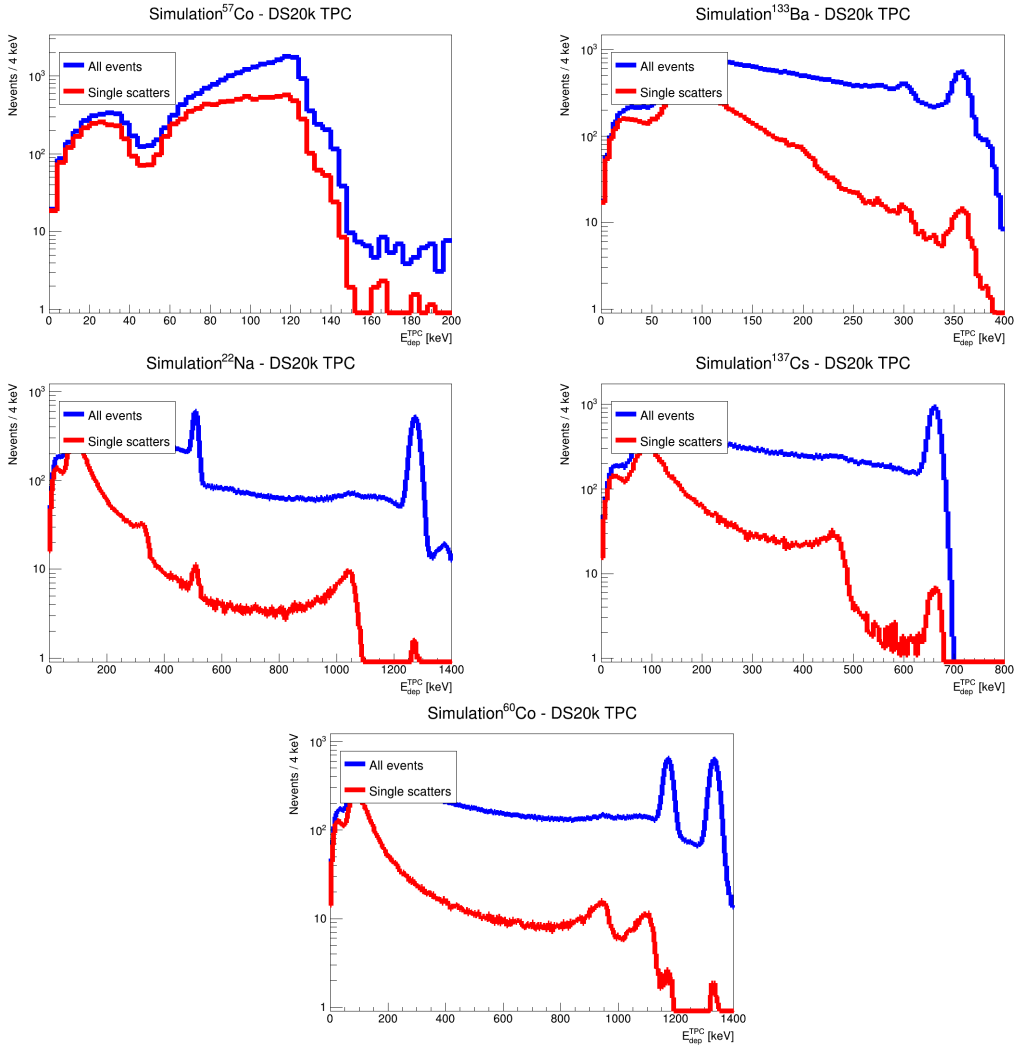


Figure 9: Number of events measured inside the TPC for five sources of photons (placed on the side of the TPC) as a function of the energy deposited in the TPC (keV). From left to right and top to bottom : ^{57}Co , ^{133}Ba , ^{22}Na , ^{137}Cs , ^{60}Co . The integral of each red curve is 10,000 (these spectra are normalised to 10,000 SS events). The spectra are log-scaled and have a 4 keV binning. The expected energy resolution of DarkSide-20k is applied.

3 SIMULATION STUDIES

3.2 Calibration with ER sources

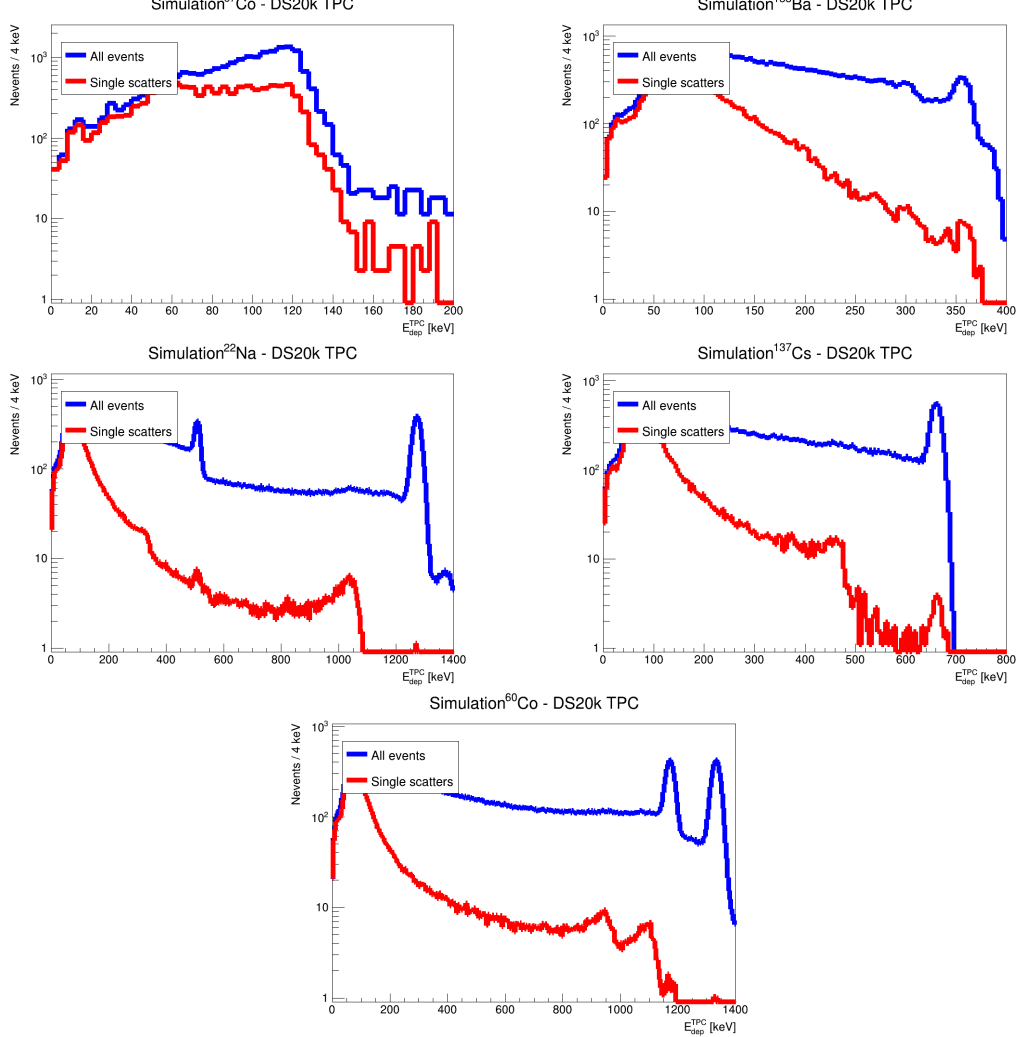


Figure 10: Number of events occurring inside the TPC for five sources of photons (situated at the bottom of the TPC) as a function of the energy deposited in the TPC (keV). From left to right and top to bottom: ^{57}Co , ^{133}Ba , ^{22}Na , ^{137}Cs , ^{60}Co . The integral of each red curve is 10,000 (these spectra are normalised to 10,000 SS events). The spectra are log-scaled and have a 4 keV binning. The expected energy resolution of DarkSide-20k is applied.

274 However, calibration could be made easier using ER single scatters with their energy
 275 inside the peaks of the spectra of the source. There isn't an online trigger permitting
 276 to directly detect single scatters ER (interesting events). Thus, the signal reconstruction
 277 system will be saturated by any type of events (single scatters or not, any energy photons:
 278 events we are not necessarily interested in).

Source	^{57}Co	^{133}Ba	^{22}Na	^{137}Cs	^{60}Co
Energy (keV)	122	356	511	662	1173
Activity (side) (kBq)	18	1.9	0.36	2.2	0.36
Activity (bottom) (kBq)	100	5.0	0.67	4.6	0.6
Duration of calibration (h)	3.84	18.72	23.52	36	74.4

Table 6: Activity needed and time estimation for the ER calibration using 1,000 SS in the energy peak and for the five previously presented sources of photons. This is made in the assumption that there isn't any online trigger. In such conditions, the time needed to perform the ER calibration run without online trigger is roughly one full week per tube.

279 Table 6 presents the results for the calibration duration to reach 1,000 SS in the
 280 peak, source by source and focusing on the gold plated events. With the previous set of
 281 hypothesis, the calibration should last one full week. This is reasonable, even considering
 282 calibration runs made to check the time stability of the detector response (such runs will
 283 take place during the data taking time). Within this time slot, it is possible to reach
 284 energy peaks with the shape of the ones on Figures 11 & 12 (respectively made on the
 285 side and at the bottom of the TPC), where the number of events per 4 keV are presented
 286 vs the energy. The integral of each peak signaled by dashed lines is 1,000. These spectra
 287 would permit a rather fast ER calibration, yet still correctly usable.

288 Taking 10,000 SS events (leading to statistical errors down to 1%) in each source
 289 position, multiplies by ten the calibration duration (making it last 2.75 months straight).

3 SIMULATION STUDIES

3.2 Calibration with ER sources

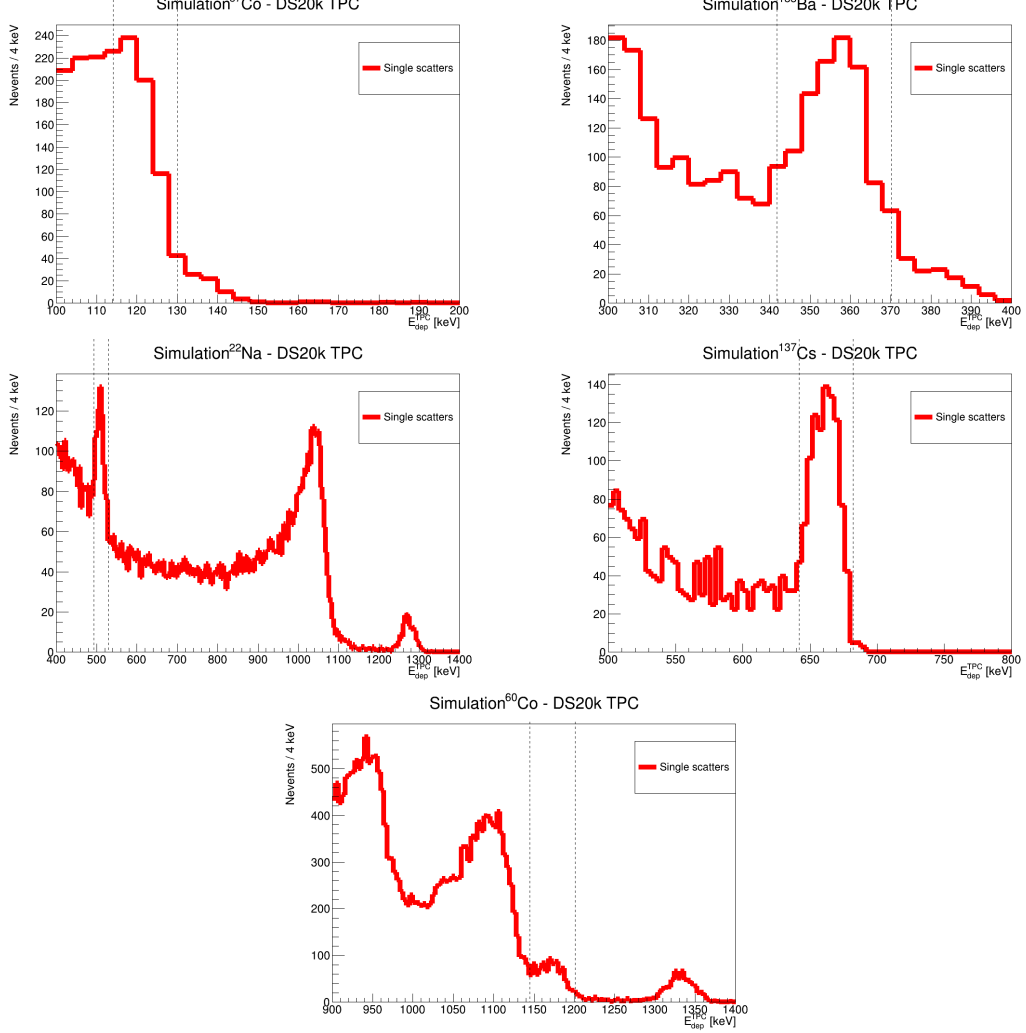


Figure 11: Number of events occurring inside the TPC after exposure of five sources of photons (placed on the side of the TPC) as a function of the energy deposited in the TPC (keV). From left to right and up to down : ^{57}Co , ^{133}Ba , ^{22}Na , ^{137}Cs , ^{60}Co . The spectra are zoomed on the energy peaks, and normalised so that there are 1,000 SS in the peak (depicted by the dashed lines). Prospective energy resolution of DarkSide-20k is applied.

3.2 Calibration with ER sources

3 SIMULATION STUDIES

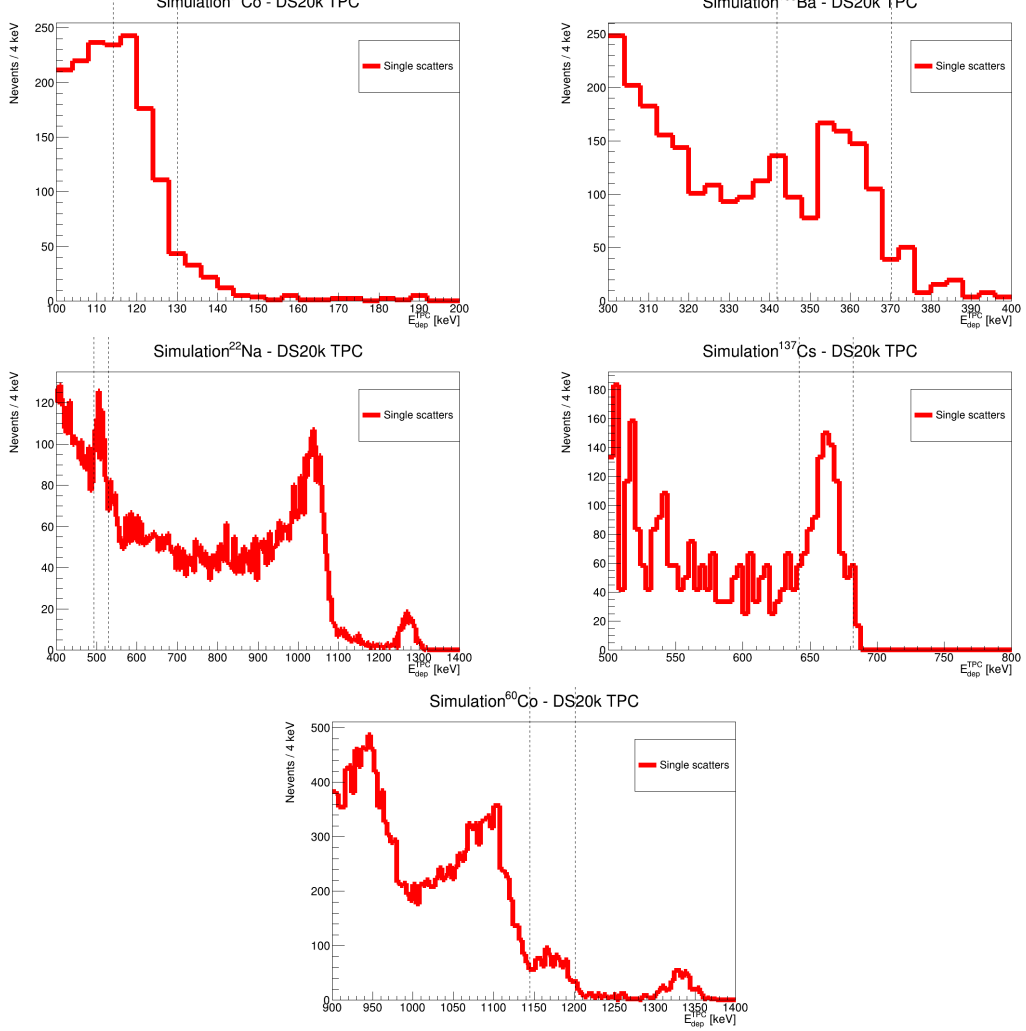


Figure 12: Number of events occurring inside the TPC after exposure of five sources of photons (placed at the bottom of the TPC) as a function of the energy deposited in the TPC (keV). From left to right and up to down : ^{57}Co , ^{133}Ba , ^{22}Na , ^{137}Cs , ^{60}Co . The spectra are zoomed on the energy peaks and normalised so that there are 1,000 SS in the peak (depicted by the dashed lines). Prospective energy resolution of DarkSide-20k is applied.

²⁹⁰ ^{241}Am (59.5 keV) and ^{109}Cd (88 keV) were studied because they can provide photons
²⁹¹ inside the energy Region Of Interest (ROI) for the WIMP discovery. At such low energies,
²⁹² the calibration starts to be very long because the rates of ^{241}Am and ^{109}Cd are very
²⁹³ small (for all events in the TPC: 4.9×10^{-6} events/decay for ^{241}Am (side), 1.3×10^{-6}
²⁹⁴ events/decay for ^{109}Cd (bottom)). ^{241}Am is barely usable: with $1e7$ simulated events
²⁹⁵ on the side part of the tubes, only 30 did a single scatter inside the TPC, half of them
²⁹⁶ with their initial energy (contributing to the photoelectric peak). Thus, with a 100 kBq
²⁹⁷ source, the data taking would last 0.3 days per calibration point. The situation is more
²⁹⁸ favorable for the slightly more energetic ^{109}Cd source, having a pure ER SS inside the
²⁹⁹ photoelectric peak rate of 5.4×10^{-6} events/decay on the side of the TPC (3×10^{-7} at the
³⁰⁰ bottom). It is very small but might be usable and affordable to complement the other

3 SIMULATION STUDIES

3.2 Calibration with ER sources

calibration sources inside the ROI, but only on the side of the TPC. Figure 13 (top) shows the spectra one can expect performing the ER calibration with this source. Figure 13 (bottom left) can be obtained in 2.7h and Figure 13 (bottom right) in 30 minutes. With the source placed at the bottom of the TPC, the corresponding spectra would require respectively 34h and 7h.

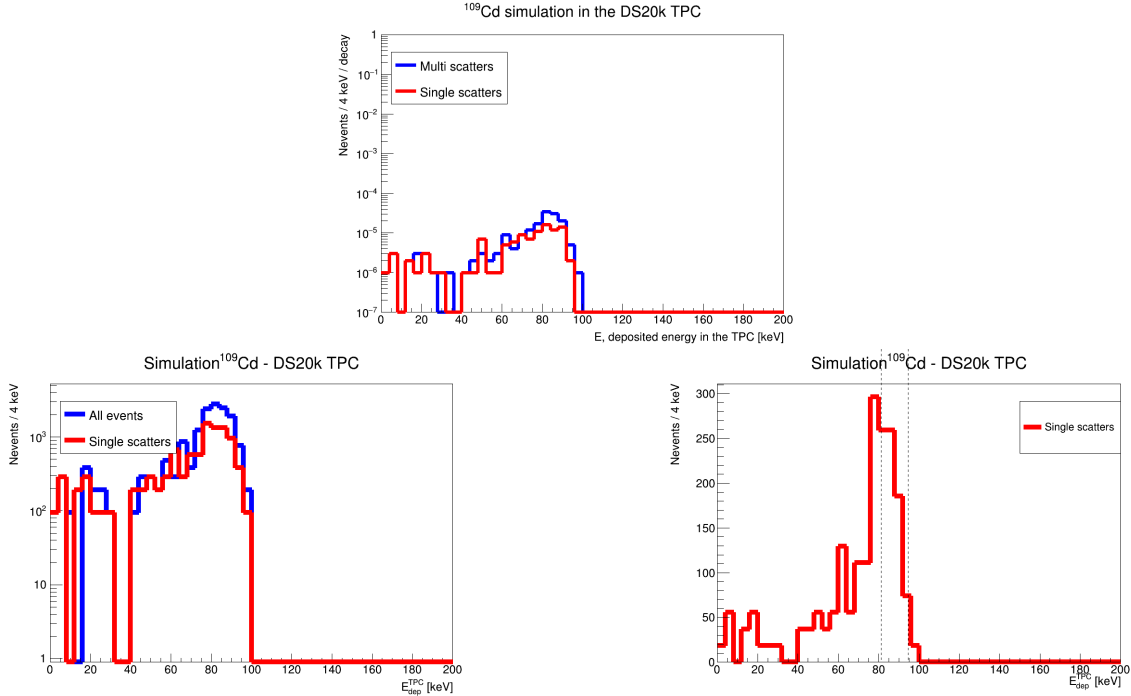


Figure 13: Top: Rate of events per 4 keV and per decay of the ^{109}Cd photon source as a function of the energy deposited in the TPC (keV). Bottom left: Number of events per 4 keV as a function of the energy deposited in the TPC (keV). The blue curve represents all events appearing inside the TPC when ^{109}Cd photon source is positioned on the side of the TPC, the red one represents the single scatters. The spectrum is normalised in order to have 10,000 SS. Bottom right: Number of events per 4 keV as a function of the energy deposited in the TPC (keV). The red curve represents all SS events appearing inside the TPC when ^{109}Cd photon source is positioned on the side of the TPC. The spectrum is normalised in order to have 1,000 SS between the dashed lines which delimiter the photoelectric peak. Prospective DS20k resolution is applied in each case.

An hypothesis to reduce the duration of the calibration is to have an online trigger, permitting to directly select gold plated events and thus saturate the DAQ system with the latter. However, all other (non interesting) events (blue curves on photon spectra) are several orders of magnitude higher in rates than gold plated events. They will still be present in the TPC and create pile-ups- which would also alterate the calibration. Furthermore, the total drift time of an electron (producing S2 signal) inside the full length of the TPC is 4 ms, which corresponds to a DAQ frequency of 200 Hz. If one still wants to have quicker calibration runs, it is possible to only focus on S1. The DAQ readout is not constrained anymore by the 4 ms drift time. S1 does not carry the whole energy of one event (it carries only 80%), but it can still provide useful information on the detector response's linearity and its time stability.

3.3 Calibration with NR sources

WIMPs are expected to produce pure nuclear recoil single scatters (pure NR SS) as they merely interact with ordinary matter and should be heavy ($m_\chi \approx 100 \text{ GeV}/c^2$ [6]). This is why such events should be carefully calibrated and studied before data taking in order to be able to distinguish between signal events and neutron background. We define the Region Of Interest (ROI) as the expected energy deposit for a WIMP, $E_{ROI} = [30, 200] \text{ keV}_{nr}$. [7]

In this section, we consider neutron emitters and simulate neutron energy deposit with AmBe and AmC sources and a Deuteron-Deuteron neutron generator(DD gun). AmBe (resp. AmC) provides neutrons with an initial energy between 0.2 and 12 MeV (resp. 2 and 7 MeV), following the spectra of Figure 14. Neutrons emitted by the two radioactive sources are accompanied by photons. DD gun provides monochromatic neutrons of 2.45 MeV. As of today, no small enough DD gun to fit the pipes has been produced.

On Figures 15 & 16, neutrons energy spectra are shown for energies of interaction below 200 keV_{nr} respectively on the side and at the bottom of the TPC. The study was made in two cases: for all pure NR events and for pure NR which interacts through a single scatter. A more quantitative analysis leads to the rates of events depicted in table 7.

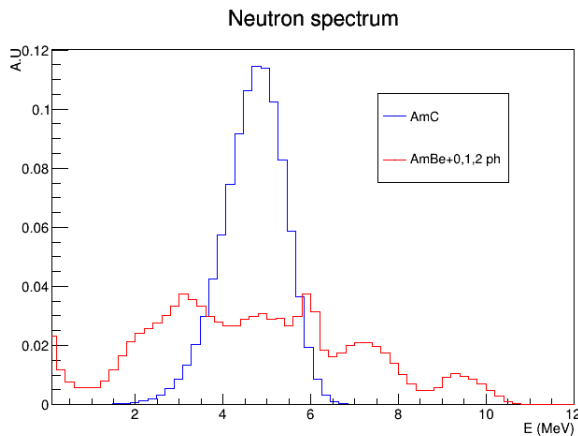


Figure 14: Neutron energy spectra when emitted by the AmC (blue curve) and AmBe (red curve) sources.

3 SIMULATION STUDIES

3.3 Calibration with NR sources

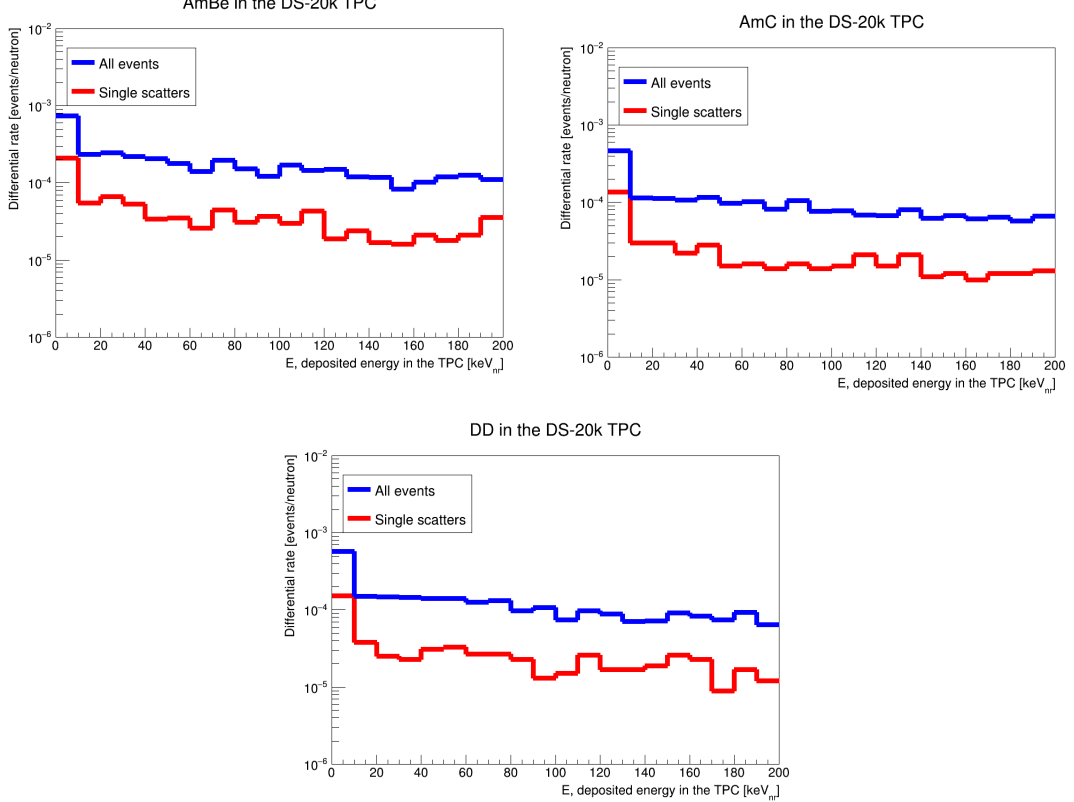


Figure 15: Rates of events per decay as a function of the energy deposited in the TPC (keV_{nr}) for three sources of neutrons (from left to right : AmBe ($E \in [0.2, 12]\text{MeV}$) , AmC ($E \in [2, 7]\text{MeV}$ and DD gun ($E = 2.45\text{ MeV}$)) placed at 3 cm from the side of the TPC.

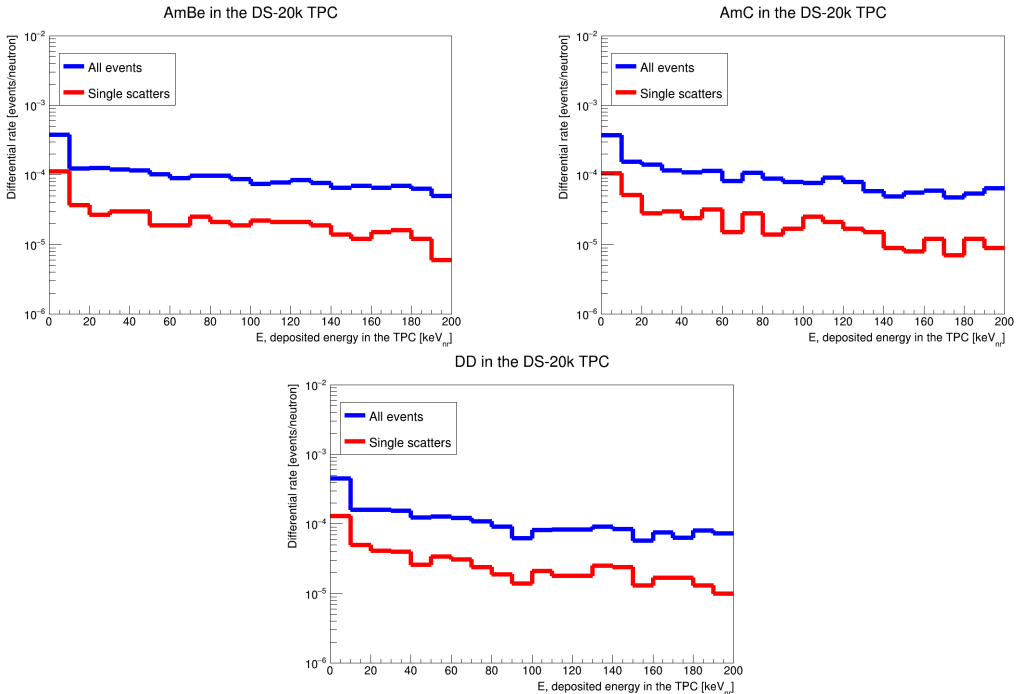


Figure 16: Rates of events per decay as a function of the energy deposited in the TPC (keV_{nr}) for three sources of neutrons (from left to right : AmBe ($E \in [0.2, 12]\text{MeV}$) , AmC ($E \in [2, 7]\text{MeV}$ and DD gun ($E = 2.45\text{ MeV}$)) placed at 1 cm under the bottom of the TPC.

3.3 Calibration with NR sources

3 SIMULATION STUDIES

Source	AmBe	AmC	DD gun
Initial energy (MeV)	[0.2, 12]	[2, 7]	2.45
Rates side (events/decay)	1.1×10^{-3}	6.4×10^{-4}	6.5×10^{-4}
Rates bottom (events/decay)	6.5×10^{-4}	6.1×10^{-4}	6.4×10^{-4}

Table 7: Rates of pure NR single scatters events detected in the TPC per decay of the calibration source inside the pipe- on the side and at the bottom of the TPC.

The rates are quite low, which is a caveat for NR calibration but a huge asset for background rejection in the experiment. This is the consequence of thick Gd-doped acrylic walls around the TPC. Indeed, with such walls producing photons accompanying calibration neutrons, having pure NR becomes a challenge. First, consider the 3 sources AmBe, AmC and DD gun, only 54-65 % of initial emitted neutrons produce a recoil (of any type) in the TPC. Among these events, about 6-10 % is at least composed of one NR -that is already only 3-6 % of the initial emitted neutrons by the source. Yet, in our study, we are interested in pure NR single scatters. Pure NR represent 7-16 % of events having at least one NR, i.e. 0.4-0.6 % of initial events. In the end, between 0.06 % and 1 % of the initial emitted neutrons are retrieved as pure NR single scatters events in the TPC (anywhere and of any energy).

In addition, if one wants to scan the Region of Interest (RoI) and the Fiducial Volume (FV) cuts, these final rates decrease by a factor ≈ 2 (between 1.75 and 2.4) when applying the selection of energy inside the RoI. Applying the FV cut, the rates decrease by a factor ≈ 9 (from 8.0 to 9.9) on the side of the TPC (the fiducial volume begins 30 cm away from the side walls) and by a factor ≈ 30 (between 26.5 and 32) at the bottom, where the fiducial volume is 70 cm above the lower wall.

With the same set of hypothesis as for the ER calibration time estimation, one can perform another time estimation for NR calibration. Results are quantified in table 8. About one week is needed for each source to reach 10,000 pure NR SS events.

Source	AmBe	AmC	AmLi	DD gun
Initial energy (MeV)	[0.2, 12]	[2, 7]	[0,2]	2.45
Activity (side) (kBq)	0.14	0.15	–	0.19
Activity (bottom) (kBq)	0.18	0.18	–	0.23
Duration of calibration (day)	8	8	–	10

Table 8: Activity needed and time estimation for the NR calibration (asking for 10,000 pure NR SS events) and for the three previously presented sources of neutrons. The overall time needed to perform the NR calibration run is four weeks straight.

Two possible modifications could be considered in the future to increase the rate:

356 **A window in the wall** Create a window in the TPC wall (reducing the thickness of
357 the wall by 10 cm on a 10x10 cm^2 square). It would permit the rates of events to increase
358 up to twice the original ones.

359 **Study at z = -150 cm** The side walls at the very bottom of the TPC (from the floor to
360 60 cm above) are thinner in Gd loaded acrylic. Indeed, there the 15 cm thick Gd loaded
361 acrylic walls splits into 10 cm of Gd loaded acrylic and 5 cm of normal acrylic. This could
362 permit to save some events if the calibration was done there. To show whether it would
363 be useful to calibrate down there, a simulation was made at z = - 150 cm (approximately
364 in the middle of this special part of the wall), leading to an increase of a factor ≈ 2 .

3.4 Light collection efficiency in the veto buffer

The calibration pipes are inside the veto buffer, reducing the light collection efficiency (LCE) in the veto. This effect was studied by simulating 1,000,000 events - an event being the release of 1,000 isotropic photons of 128 nm (9.7 eV) in the veto volume. The simulations considered five cases for the optical surface of the pipes as available in g4ds: either the pipes are untreated stainless steel (UT), either the pipes are electro-polished stainless steel (EP), either they are TPB-coated (TPB, with a reflector layer between the pipe and the TPB), either they are PEN-coated (PEN, with a reflector layer between the pipe and the PEN) or they are only coated by the reflector foil, called ESR. Note that this section presents results with stainless steel pipes, which is the material foreseen. If titanium had been used instead, we have checked that this would not have changed the conclusion: the best solution is still to wrap the pipes with ESR, and the performances are very similar.

In order to study the light collection efficiency, the following was considered:

- In a 3D view: four regions of the veto are taken into account: the full veto buffer, its bottom part, its top part and its side-part.
- In a 2D cut-view: two octants of the circle were compared: one without pipes (between angles of $\frac{3\pi}{8}$ and $\frac{5\pi}{8}$) and one with a portion of the pipes (between angles of $\frac{\pi}{8}$ and $\frac{3\pi}{8}$ - see figure 17).

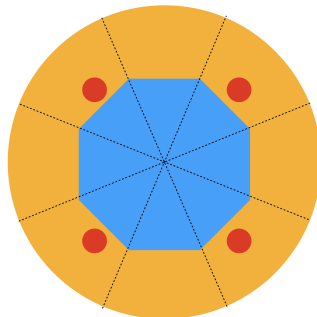


Figure 17: Scheme of the TPC (blue) with the veto buffer around it (yellow) and pipes inside (red). The scheme is not at scale. Separations of the veto buffer into eight sub-regions are depicted: four with pipes and four without.

3 SIMULATION STUDIES

3.4 Light collection efficiency in the veto buffer

LCE	Full Veto Buffer (mean) (%):					Octants with pipes (mean) (%):					Octants without pipes (mean) (%):				
	UT	EP	TPB	PEN	ESR	UT	EP	TPB	PEN	ESR	UT	EP	TPB	PEN	ESR
Optical Boundaries															
All	3.66	3.72	3.97	3.94	4.00	3.59	3.67	3.94	3.90	3.99	3.73	3.78	4.00	3.97	4.01
Side	3.72	3.78	4.04	4.00	4.06	3.60	3.68	3.99	3.95	4.06	3.85	3.88	4.08	4.05	4.07
Top	3.85	3.89	4.03	4.01	4.03	3.84	3.88	4.02	4.01	4.03	3.86	3.90	4.04	4.02	4.04
Bottom	3.43	3.51	3.85	3.80	3.90	3.40	3.50	3.83	3.77	3.89	3.46	3.54	3.87	3.83	3.90

Table 9: Table of the LCE in three 2D cut-view-areas of the veto buffer: an average inside the full veto, in the four octants where pipes are and in the four octants where pipes are not. For each of these three considerations, the table shows the LCE in four volumes: inside the whole volume, on the side, the top part and the bottom part of the veto. This is done for five optical boundaries: untreated steel (UT), Electro-polished steel (EP), ESR-wrapped + TPB-coated pipes (TPB), ESR-wrapped + PEN-coated pipes (PEN) and ESR-only-wrapped pipes (ESR). Errors on this numbers are less than 1×10^{-2} .

LCE	Full Veto Buffer (Mean):
All	4.04 %
Side	4.09 %
Top	4.05 %
Bottom	3.97 %

Table 10: Table of the maximum LCE reachable in the veto buffer (case without pipes). Errors on this numbers are less than 1×10^{-2} .

As one can see in the table 9, the light collection efficiency is $\approx 3\text{-}4\%$ in each case. The sectors with pipes have a lower efficiency than the ones without pipes as one can expect (the light can be absorbed by the tubes).

As a reference study, the light collection efficiency without the calibration system in the veto was taken (see table 10). It can reach an efficiency of $\approx 4.04\%$. Thanks to this last study, it is possible to compute the relative loss of efficiency as an average in the veto, computed as

$$\frac{LCE_{\text{without-pipes}}^{\text{Full}} - LCE_{\text{UT-EP-TPB-PEN-ESR}}^{\text{Full}}}{LCE_{\text{without-pipes}}^{\text{Full}}} \quad (1)$$

and in the pipes regions, computed as

$$\frac{LCE_{\text{without-pipes}}^{\text{Pipes-octants}} - LCE_{\text{UT-EP-TPB-PEN-ESR}}^{\text{Pipes-octants}}}{LCE_{\text{without-pipes}}^{\text{Pipes-octants}}} \quad (2)$$

Tables 11 and 12 store the results. The best situation is to have ESR-coated pipes, where the efficiency is the highest (between 3.89% and 4.07%). This is consistent with the reflectivity of the different surfaces (see Fig 42 of TDR [1]), with a reflectivity of ESR foils at the level of 98% for 420 nm photons. The presence of the pipes that are wrapped with an ESR foil do reduce the inclusive veto LCE by about 1% (up to 2% in sectors where the tubes are).

3.4 Light collection efficiency in the veto buffer

3 SIMULATION STUDIES

$\frac{\Delta LCE}{LCE}$	UT (%)	EP (%)	TPB (%)	PEN (%)	ESR (%)
All	9.4	7.9	1.7	2.5	0.91
Side	9.0	7.6	1.2	2.2	0.75
Top	4.9	4.0	0.5	0.99	0.32
Bottom	14	12	3.0	4.3	1.9

Table 11: Relative loss of the average LCE. The reference is the LCE in the case where there are no tubes in the veto.

$\frac{\Delta LCE}{LCE}$	UT (%)	EP (%)	TPB (%)	PEN (%)	ESR (%)
All	11	9.2	2.5	3.5	1.1
Side	12	10	2.4	3.4	0.95
Top	5.2	4.2	0.7	0.99	0.31
Bottom	14	12	3.5	5.0	2.0

Table 12: Relative loss of LCE in pipes octants. The reference is the LCE in the case where there are no tubes in the veto.

Finally, there is an asymmetry between octants induced by the pipes which was studied because the veto needs to be as uniform as possible. To study the effect, the ratio

$$\frac{LCE^{Octants-Without-Pipes} - LCE^{Octants-With-Pipes}}{LCE^{Octants-Without-Pipes}} \quad (3)$$

was computed, the results are stored in table 13. The asymmetry is $\approx 0.3\%$ for pipes treated with a reflector ESR. Such asymmetry is not of concern for the operation of the veto.

403

Asymmetry	UT (%)	EP (%)	TPB (%)	PEN (%)	ESR (%)
All	3.8	2.9	1.5	2.0	0.3
Side	6.5	5.2	2.2	2.0	0.3
Top	0.5	0.5	0.5	0.2	0.05
Bottom	1.7	1.1	1.0	2.0	0.2

Table 13: Asymmetry between octants computed as the relative difference of light collection efficiency between octants where pipes are not and octants where pipes are - for the five options of optical boundaries of the pipes.

All above results with ESR-coated tubes have been repeated for 5 cm diameter tubes instead of 3, to check the impact of larger tubes. The relative loss of LCE for the inclusive case (all sectors) increases from 0.91% to 1.4%. For all sectors with pipes it goes from 1.1% to 1.7%. The inclusive asymmetry between the sectors increases from 0.3% to 0.6%. We can conclude that for 5cm tubes, the impact on LCE is still very much acceptable.

3.5 Background induced by the guide tube system

The following results have been obtained primarily for 3 cm Titanium tubes, but have been updated for stainless steel, for which all numbers will be given. The conclusions are the same for both materials. Two different types of screened stainless steels have been considered, one noted LZ and the other one noted ArDM, being considered respectively as best (resp. worst) case scenarii. Results in this section are given for LZ stainless steel, and results for ArDM stainless steel are available in appendix E. Note that for larger pipes of 5 cm diameter, all background rates presented below would increase by a factor of $\times 1.7$ and would still be well within the allowed limits.

The guide tube material can be contaminated by radioactive elements such as ^{238}U , ^{232}Th ... [1]. When they decay, these radioactive elements will produce photons and neutrons which might penetrate the TPC and produce ER and NR backgrounds. In the current design, the calibration pipes are made of 30 kg stainless steel (17 kg of Titanium was also an option). The impact of the background from the pipes has been studied and compared to the budget required by the DarkSide collaboration.

Table 14 (resp. Table 15) gives the list of the radioactive elements polluting the Titanium (resp. stainless steel) of the pipes.

Element	^{238}U Upper	^{238}U Middle	^{238}U Lower	^{232}Th	^{235}U	^{40}K	^{46}Sc
Contamination (mBq/kg)	8	0.12	80	0.12	0.37	0.6	3.1
Photon producer ?	Yes	Yes	Yes	Yes	Yes	Yes	Yes
Neutron producer ?	Yes	Yes	Yes	Yes	Yes	No	No
Neutron yield (neutron/decay)	4.9×10^{-9}	2.6×10^{-6}	1.6×10^{-8}	6.5×10^{-6}	2.6×10^{-6}	No	No

Table 14: For Titanium: contamination sources inside the pipes and their respective contamination levels (mBq/kg), background production and neutron yield. [1]

Element	^{238}U Upper	^{238}U Middle	^{238}U Lower	^{232}Th	^{235}U	^{40}K	^{60}Co	^{137}Cs
Contamination (mBq/kg)	1	0.72	1	0.83	0.046	0.49	3.1	0.86
Photon producer ?	Yes	Yes	Yes	Yes	Yes	Yes	Yes	Yes
Neutron producer ?	Yes	Yes	Yes	Yes	Yes	No	No	No
Neutron yield (neutron/decay)	1.1×10^{-9}	4.8×10^{-7}	1.06×10^{-9}	1.8×10^{-6}	3.7×10^{-7}	No	No	No

Table 15: For Stainless steel, assuming LZ-type stainless steel: contamination sources inside the pipes and their respective contamination levels (mBq/kg), background production and neutron yield.

These radioactive elements will produce ER and NR background. These rays are isotropically radiated from the whole pipe, around the TPC. Hence, only a fraction of photons and neutrons emitted from the pipe will enter the TPC. 10 million events were simulated for each element (with their full chain radioactive decays), the fraction of their

3.5 Background induced by the guide tube system

3 SIMULATION STUDIES

431 energy deposited in the TPC was calculated and cuts were applied. If no event passes
 432 the cuts, an upper limit at < 2.3 events is set, corresponding to the limit of a poissonian
 433 distribution with mean zero at 90% C.L. After all these steps, the counts are normalized
 434 to the radioactive contamination of the material (see table 14), the mass of the tubes and
 435 the time exposure (ten years of experiment).

436 3.5.1 NR background

437 The study first examines the NR background case. Only ^{232}Th , ^{238}U and ^{235}U produce
 438 neutrons, through (α , n) reactions. The selected events in the NR study are pure NR
 439 events, doing single scatters in the fiducial volume, in the energy region of interest for
 440 WIMP search in NR channel ($30 \text{ keV}_{nr} < E < 200 \text{ keV}_{nr}$ [7], and a veto cut ($E_{veto} <$
 441 200 keV_{nr}). The normalisation also includes the production rate of neutrons by the
 442 contaminating radioactive elements. These rates are shown in the last line of Table 14
 443 (resp. Table 15) for Titanium (resp. stainless steel).

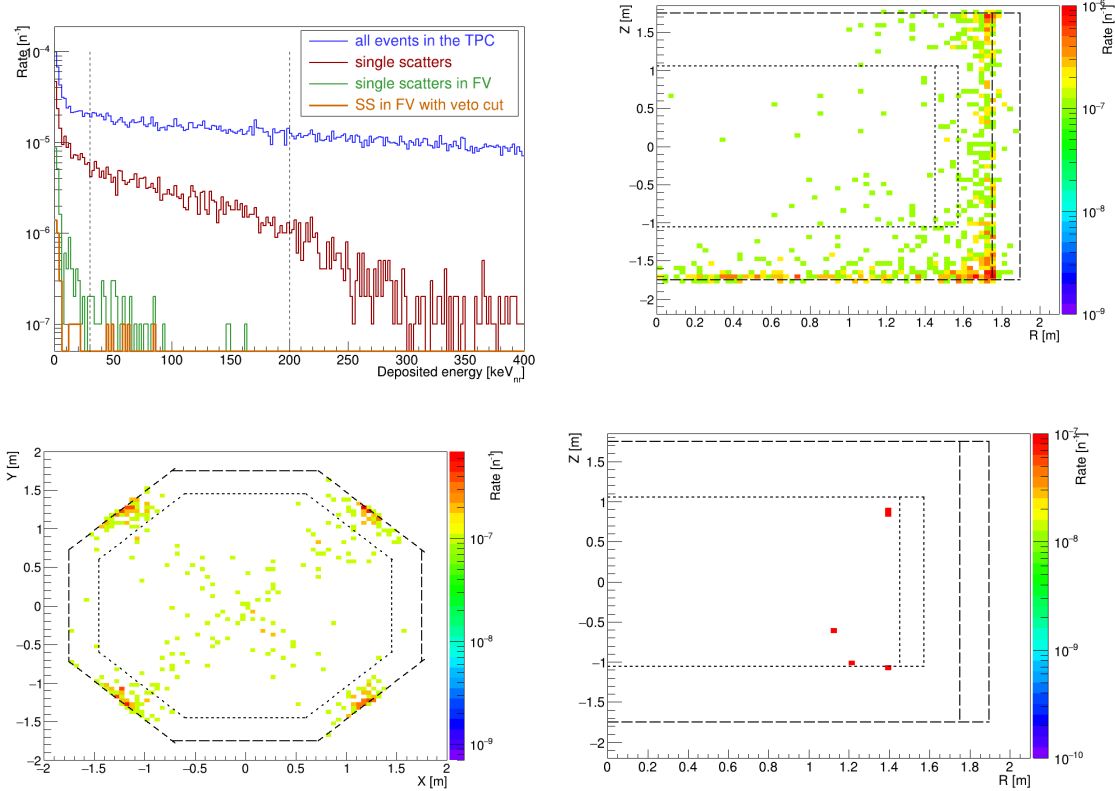


Figure 18: Up left : energy spectrum of NR events induced by the presence of ^{232}Th in the guide tube system (titanium) in four cases : all events, single scatters, single scatters in FV and single scatters in FV after the veto cut. Up right : geometric view of NR background events (from ^{232}Th decay) in the TPC in the R^2Z plane, after all cuts except ROI & FV. Down left : cut-view of NR background events (from ^{232}Th decay) in the TPC in the XY plane, after all cuts except FV. Down right: geometric view of NR background events (from ^{232}Th decay) in the TPC in the RZ plane, after every cuts.

3 SIMULATION STUDIES

3.5 Background induced by the guide tube system

As presented on Figure 18- top right and bottom-left that events are localised near the pipes, a few events are in the fiducial volume. As seen in Figures 18-up left and 18-down right, five events for Titanium (4 for stainless steel) resist the cuts after 10^7 events simulated per radio nuclide. Seven events for Titanium (4 for stainless steel) resisted the cuts for ^{238}U . The final quantitative results of the study are shown in the table 16 (resp. Table 17) for Titanium (resp. stainless steel) tubes, for the three sources. ^{235}U 's background level has an asterisk because this radio-contaminant isn't coded in g4ds. We estimated an amount of background taking the emission spectrum of ^{238}U and normalised it with ^{235}U 's parameters.

Element	^{238}U Upper	^{238}U Middle	^{238}U Lower	^{232}Th	^{235}U
Contamination (mBq/kg)	8	0.12	80	0.12	0.37
Neutron yield (neutron/decay)	4.9×10^{-9}	2.6×10^{-6}	1.6×10^{-8}	6.5×10^{-6}	2.6×10^{-6}
Events/10years	1×10^{-7}	1×10^{-6}	5×10^{-6}	2×10^{-6}	$3 \times 10^{-6} *$

Table 16: NR background rates induced by the radioactive contamination of the Titanium pipes after normalisation (which includes the neutron production rate of the three radioactive elements). [1]

Element	^{238}U Upper	^{238}U Middle	^{238}U Lower	^{232}Th	^{235}U
Contamination (mBq/kg)	1	0.72	1	0.83	0.046
Neutron yield (neutron/decay)	1.1×10^{-9}	4.8×10^{-7}	1.06×10^{-9}	1.8×10^{-6}	3.7×10^{-7}
Events/10years	4.0×10^{-9}	1.3×10^{-6}	4.0×10^{-9}	5.7×10^{-6}	$6.0 \times 10^{-8} *$

Table 17: NR background rates induced by the radioactive contamination of the Stainless Steel pipes, assuming LZ-type stainless steel, after normalisation (which includes the neutron production rate of the three radioactive elements).

This study shows that the background from impurities in the pipes produce around 10^{-5} events for 10 years of data taking (both for Titanium and Stainless Steel pipes). This result is fully compatible with the ones of the TDR, expecting 9.9×10^{-4} events from neutrons after the $200 \text{ t} \times \text{yr}$ exposure for 980 kg of Titanium (coming from the vessel). Considering that the background budget is settled at 0.1 events per 10 years, the NR background induced by the calibration system is fully negligible (it is more than four orders of magnitude less than the requirements). This low rate of events is due to the gadolinium walls which better stops neutrons than usual walls.

3.5.2 ER background

ER background has now to be analysed. All radioactive contaminants produce photons, which might produce ER signal in the TPC. This time, the set of cuts applied to the ER background analysis is: having single scatters inside the energy Region Of Interest

3.5 Background induced by the guide tube system

for the WIMP discovery ($7.5 \text{ keV}_{ee} < E < 50 \text{ keV}_{ee}$) and in DS20k's Fiducial Volume (SS + ROI + FV). Figure 19-top shows the evolution of the energy distribution of ^{238}U 's ER background events cuts after cuts. Figure 19 bottom (left and right) shows that the background is located around the pipes and at the borders of the TPC (still in ^{238}U case yet all radio contaminants analysis lead to the same result).

3 SIMULATION STUDIES

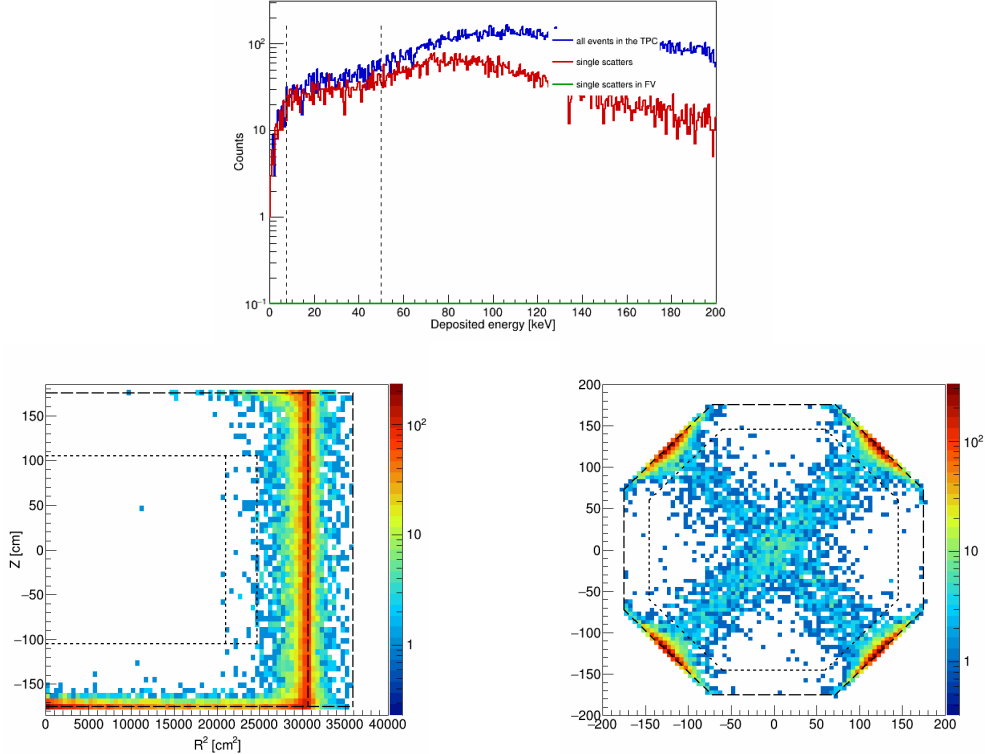


Figure 19: Up: energy spectrum of ER events induced by the presence of ^{238}U the guide tube system (titanium) in three cases : all events, single scatters and single scatters in FV. The prospective resolution of the detector is applied. Bottom left: geometric view of ER background events (from ^{238}U decay) in the TPC in the R^2Z plane, before the FV cut. Bottom right : cut-view of ER background events (from ^{238}U decay) in the TPC in the XY plane, before the FV cut.

Results are stored in Table 18 (resp. Table 19) for Titanium (resp. stainless steel) tubes. There are only upper limits as no event survived the cuts. The results shown in the table are the ones before the S2/S1 requirement and the PSD (which will bring another 10^7 to 10^8 rejection). To conclude, the ER background induced by the tubes is fully negligible (both for Titanium and Stainless Steel pipes). These results are compatible with what is mentioned in the TDR for the ER background induced in the TPC by the 980 kg of the titanium vessel.

3 SIMULATION STUDIES

3.5 Background induced by the guide tube system

Element	^{238}U Upper	^{238}U Middle	^{238}U Lower	^{232}Th	^{235}U	^{40}K	^{46}Sc
Contamination (mBq/kg)	8	0.12	80	0.12	0.37	0.6	3.1
Events/10years	< 10	< 0.2	< 100	< 0.2	< 0.5	< 0.7	< 4

Table 18: ER background rates induced by the radioactive contamination of the Titanium pipes after normalisation. [1]

Element	^{238}U Upper	^{238}U Middle	^{238}U Lower	^{232}Th	^{235}U	^{40}K	^{60}Co	^{137}Cs
Contamination (mBq/kg)	1	0.72	1	0.83	0.046	0.49	3.1	0.86
Events/10years	< 2	< 1.5	< 2	< 2	< 0.1	< 1	< 7	< 2

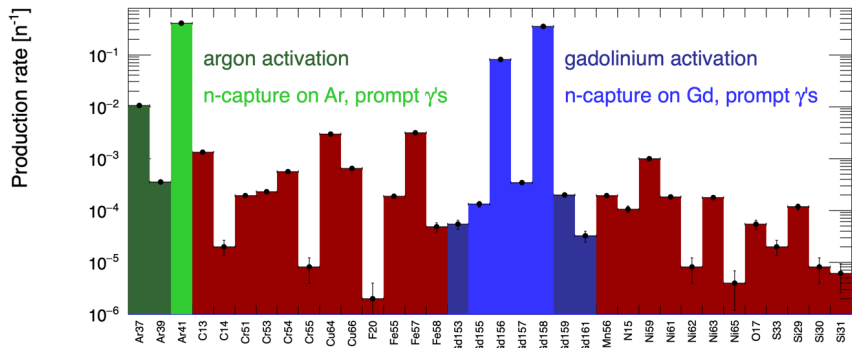
Table 19: ER background rates induced by the radioactive contamination of the Stainless Steel pipes, assuming LZ-type stainless steel, after normalisation.

477 It is also important to make sure this background won't be too important before all
 478 off-line cuts to certify that it won't pollute the DAQ systems of the TPC and of the veto.
 479 Between 1 and 17 % (resp. 1 and 20 %) of the events emitted by the contaminants in the
 480 Titanium (resp. Stainless Steel) pipes will deposit energy in the TPC. This represents
 481 a rate of recorded events in the TPC between less than 0.001 Hz and 0.01 Hz (resp.
 482 between less than 0.001 Hz and 0.018 Hz). The summed TPC rate in the DAQ read-
 483 out induced by the calibration tubes is 0.02 Hz (for both Titanium and Stainless Steel),
 484 which represents 0.04% of the sum of what is presented in the TDR: it is fully negligible.
 485 Between 11.8 and 97.4 % (resp. 11.8 and 97.1 %) of events emitted by the contaminants
 486 of the Titanium (resp. Stainless Steel) pipes will deposit energy in the veto, representing
 487 between less than 0.001 Hz and 0.16 Hz (resp. between less than 0.001 Hz and 0.09 Hz) of
 488 events in the veto DAQ. The summed veto rate induced by the Titanium (resp. Stainless
 489 Steel) calibration tubes is 0.2 Hz (resp. 0.12 Hz), which represents 0.15% (resp. 0.09%)
 490 of the rate induced by all other materials in the veto, as mentioned in the TDR. The rate
 491 induced by the tubes in the veto buffer is small.

492

493 3.5.3 Neutron capture and materials activation

494 Neutron activation of detector was evaluated with MC for all sources mentioned in
 495 Section 3.3. A list of unstable isotopes produced by neutron capture is shown for a
 496 DD-generator in figure 20. While some of them de-excite quickly and result in prompt
 497 gammas (which in turn can serve calibration purposes for the veto buffers), some have
 498 long lifetimes, and might present experimental background. Of particular importance is
 499 the activation of argon, as in this case isotopes decay directly in the target volume and
 500 such events cannot be fiducialised. Note that this study has been done using a previous
 501 version of the detector veto geometry, but the same TPC argon volume. Conclusions
 502 should hence remain similar.



503 Figure 20: Isotopes produced by DD neutron capture in the detector materials. The
 504 vertical error bars represent statistical uncertainty.

503 Three activated isotopes of argon were identified, presented in table 20 with the
 504 half-life and computed production rates. The production rates for ³⁷Ar and ³⁹Ar are
 505 well below $\mu\text{Bq}/\text{kg}$ level, hence are negligible and do not present any danger for the
 506 experimental goals. Neutron capture on ⁴⁰Ar results in prompt gammas with a total
 507 energy of 6.1 MeV, concurrent with the transition to ⁴¹Ar isotope, which is radioactive
 508 and undergoes β -decay with a Q-value of ~ 2.5 MeV. It is produced in the target volume
 509 during neutron calibration at the rate of 2.6 mBq/kg/day, similar activity as expected
 510 from ³⁹Ar (0.73 ± 0.11 mBq/kg) and ⁸⁵Kr (2.05 ± 0.13 mBq/kg), however given relatively
 511 short half-life of 1.83 hours will decay within a day after the calibration run.

Table 20: Isotopes produced in the liquid argon target by neutron capture during the calibration run with a DD generator, from the Monte Carlo simulation with GEANT4.

Isotope	$T_{1/2}$	Production rate [Bq/kg/day] with a 100 neutron/sec source		
		target argon	inner veto buffer	outer veto buffer
³⁷ Ar	35.04 days	$\sim 10^{-7}$	$\sim 10^{-7}$	$\sim 1 \times 10^{-9}$
³⁹ Ar	269 years	$\sim 10^{-12}$	$\sim 10^{-12}$	$\sim 1 \times 10^{-13}$
⁴¹ Ar	109.34 min	2.6×10^{-3}	1.6×10^{-3}	3.2×10^{-5}

3.6 Neutron Veto Inefficiency

In this section, the effect of the calibration pipes s on the neutron veto efficiency is estimated. Neutrons are simulated in the topical positions with activities based on the radio purity of the corresponding material, and energies are sampled from the ^{238}U , ^{235}U , and ^{232}Th chain. In order to obtain an estimate, only neutrons originated from the TPC and Veto PDUs are simulated. After the neutrons are propagated through the detector components, energy deposits are recorded and analysis cuts are applied to obtain the number of WIMP-like events given the following calibration geometry configurations. WIMP-like events are those surviving the following cuts:

- NR Single Scatter
- Energy ER of $7.5 \text{ keV} < E_R < 50 \text{ keV}$
- Energy deposit in the fiducial volume, 20 tone fidualization
- Energy threshold cut: 50 keV for TPC and 200 keV for the veto
- TPC - Veto time window of 800 us

	PDU	vPDU
With 3cm pipes	$6.15 \times 10^{-6} \pm 5.5 \times 10^{-7}$	$1.4 \times 10^{-6} \pm 2.6 \times 10^{-7}$
With no pipes	$6.15 \times 10^{-6} \pm 5.5 \times 10^{-7}$	$1.15 \times 10^{-6} \pm 2.4 \times 10^{-7}$

Table 21: Veto Inefficiency

526 4 Hardware implementation

527 This section describes the components, integration and operation of the guide pipe
 528 system in sections 4.1, 4.2 and 4.3, respectively. Once operational, the system has to
 529 guarantee the safe inclusion and extraction of the radioactive sources and their smooth
 530 movement inside the calibration pipes.

531 The main concerns are the smooth operation at liquid argon temperature and the
 532 risks associated with ice formation. To study these two aspects, three mock-ups have
 533 been planned and are described in section 4.4. First results are also given in this section

534 4.1 Components and status

535 The four main components of the system are the guide tubes, the motors (and their
 536 associated mechanical and monitoring systems) that allow the circulation of the source,
 537 the glove boxes that allow the insertion of the source and the rope on which the source
 538 is attached. The current status of the components are given in Table 22 and detailed in
 539 this section.

	Guide Tubes	Motors		Glove boxes	Ropes
		Hardware	Software		
Number	2	4	1	4	4
Final Design	completed*	completed	being finalized	in dev	completed
Availability	2024	03/22	Q2 2023	Q4 2023	2022

Table 22: Components of the calibration system and status of completion (01/2023). *
 Only the final diameter is still under discussion.

540 4.1.1 Guide tube

541 The baseline for the calibration system consists in two orthogonal pipes of 3 cm inter-
 542 nal diameter and 1.5 mm thickness. The diameter is sufficient for radioactive sources and
 543 may need to be enlarged in order to accept DD-gun as a neutron generator. Screening of
 544 the raw material is needed in order to keep the background contributions from the pipes
 545 to < 0.01% of the global level of estimated background of 0.10 events in 200 tonne×year
 546 exposure (see section 3.5). The surface of the pipes will be covered with a reflector in the
 547 optical volume of the Veto (see section 3.4). The pipes follow a routing along and below
 548 the TPC which is illustrated in Figure 3. Each pipe goes vertically along a lateral face of
 549 the TPC, then reaches the bottom following a bending of 40 cm curvature radius, goes
 550 to the opposite side passing by the center and finally (after a second bending) goes up
 551 vertically along the opposite lateral face of the TPC. A further set of bends is necessary
 552 for each pipe to go out through the two exits on the roof of the cryostat, away from the
 553 detector support system. In total the tube is about 20 meter with 15 bends as seen in
 554 Figure 21. A bend at the very bottom is seen, which will be present for one of the two
 555 tubes in order to allow their crossing.

556

4 HARDWARE IMPLEMENTATION

4.1 Components and status

At the exit of the cryostat top caps, the 4 tube ends will be welded to as many bellows which have the following functions: 1) guarantee leak tightness of the cryostat AAr volume 2) accommodate the mis-alignments of the tube with the penetrations on the cryostat during installation; 3) accomodate the vertical motion of the detector + SS vessel + cali system during lifting of the whole assembly with the Detector Support System 4) accomodate the vertical and horizontal shrinkage of the full assembly during filling and operation at LAr.

564

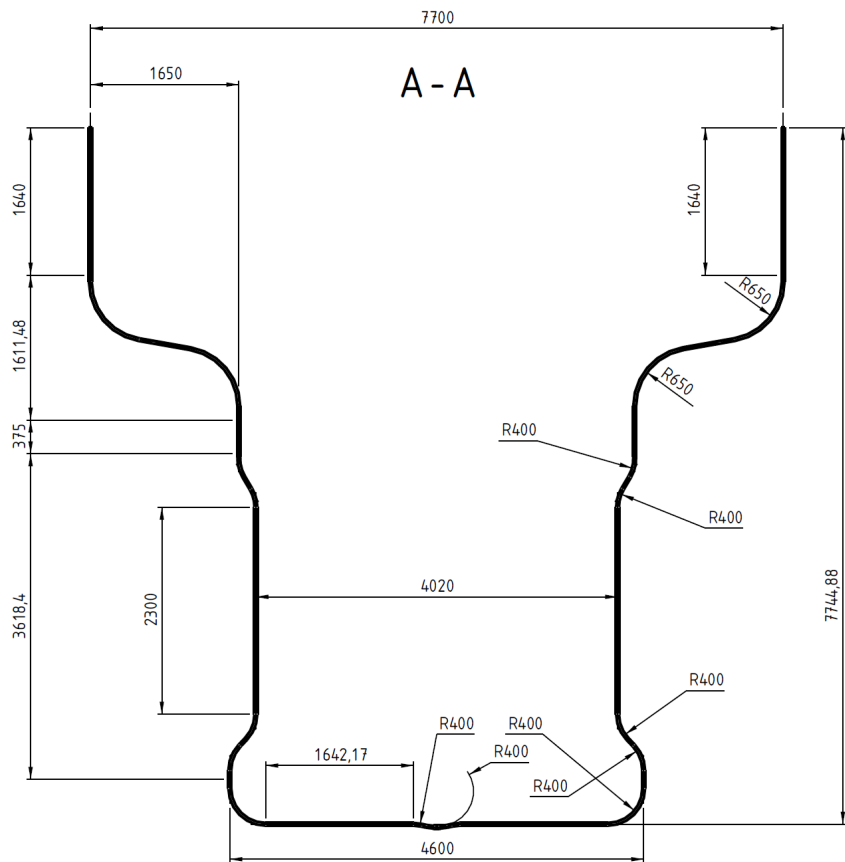


Figure 21: Full-scale view of one tube foreseen to be installed in DARKSIDE-20K calibration system.

Discussion for the procurement of the material for the two guide tube is ongoing. One option is to use the same material as for the stainless steel vessel. The bending of the guide tube will benefit from the experience of the mock-up (section 4.4). The delivery of the final tubes at Gran Sasso is expected in 2024. The screening of a sample should happen a bit before in order to validate the batch. It will depend on the option selected for the procurement. A screening test is also foreseen on a sample of the mock-up tubes in 2023.

572 **4.1.2 Motors**

573 The motor system, designed and built at Queen's University (QU), is inspired by the
 574 one operated at the SNO+ experiment. Figure 22 top shows the position of different
 575 elements of the motor : the rope, the drum, a set of pulleys, the spring with the rope
 576 at the center to limit the extent makes the tension come on gradually and allows better
 577 control, the load cell and the very low friction encoder pulley that allow the recording
 578 of the source position. On one side, the rope is directed to the cryostat. On the other
 579 side each motor is coupled to the system via a flexible shaft. The motors are controlled
 580 through a monitoring system described by the diagram represented at the bottom of
 581 the figure 22. For each motor system, a dedicated power supply (providing 24V and a
 582 current never exceeding 2A) powering a motor box which provides power and orders to
 583 the motor and link to the micro-controller board which acts as a mother board. This one
 584 is connected to the two motor boxes as well as the loadcell and encoder of each motor
 585 system. The mother board is controlled by a PC (through USB connection) running
 586 C++ program to monitor the whole system.

587 By design there are two independent ways to know the source position (motor step and
 588 encoder). If they do not agree within tolerance, the system shuts down. The tolerance is
 589 set by the rope spring constant and mechanical stiffness plus load-cell accuracy and noise.
 590 The shutdown value corresponds to a force of 40 N for the DARKSIDE-20K calibration
 591 system and could be adjusted during the run. Note that the (original) recommended
 592 value used by the SNO+ experiment was 100 N, due to heavier sources used.

593
 594 The four motors systems needed for the system have been built (mechanical parts) or
 595 purchased (motors and electronic boards). Two are presently at CPPM for tests on the
 596 mock-ups and two are at QU. Only the mechanical structures of the boxes containing the
 597 mechanical system are missing.

598 **4.1.3 Glove boxes**

599 The glove box is a mandatory element of the calibration system which will be used
 600 to attach the source to the rope before it is driven in the tubes. The left part of the
 601 figure 23 shows the result of a recent study of the glove box design. It will be used to
 602 contact companies that are foreseen to manufacture these glove boxes. The central and
 603 right parts of the figure 23 show the actual implementation of the glove boxes in the
 604 global CAD of DarkSide20K experiment. In order to assess the needs in term of size of
 605 the glove aperture, overall dimensions and geometry, a mock-up of the glove box has been
 606 made at CPPM in 2022. The figure 24 shows different views of this mock-up which has
 607 also been useful to start the brainstorming on how to fix the source to the ropes with
 608 limited risks to drop either the source or the rope inside the tube. A calibration run
 609 procedure (see section 4.3) focused on the glove box manipulation has been written. It
 610 will be adjusted when the final glove box will be tested.

611 **4.1.4 Rope**

612 The rope is 25.5 m long and has a 2 mm diameter and weight **around 1 kg**. It is
 613 attached to each motor so there is 4 ropes in total. It is made of single-braid rope of

4 HARDWARE IMPLEMENTATION

4.1 Components and status

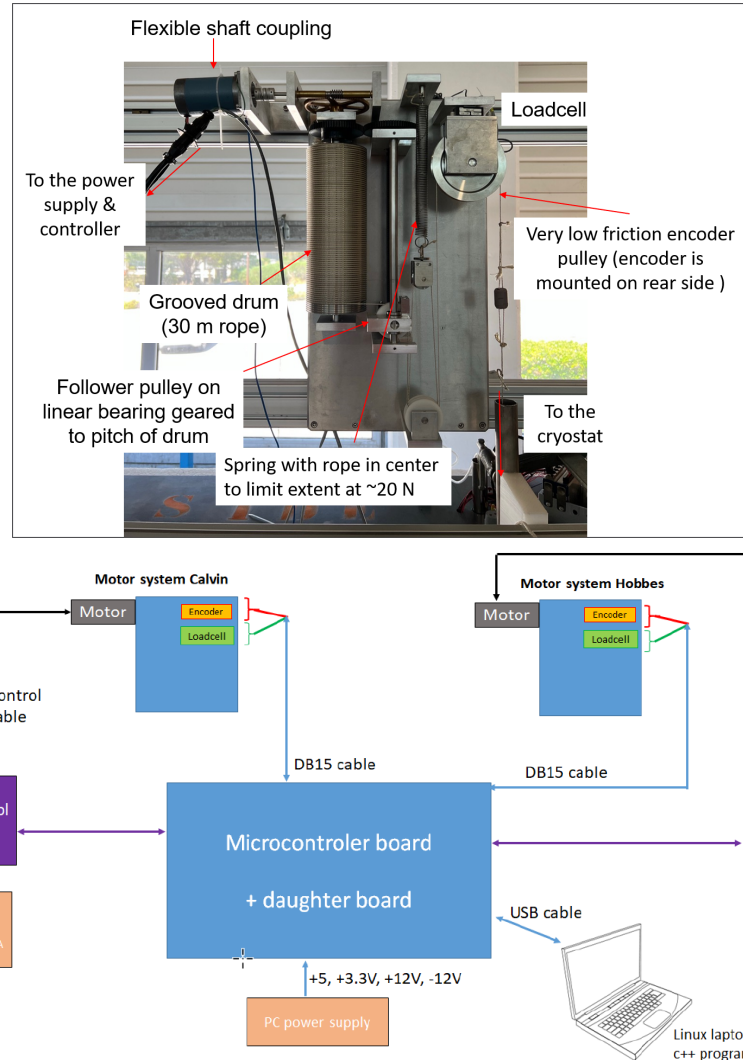


Figure 22: Top : Components of a motor box. Bottom : General view of the monitoring of the motor system.

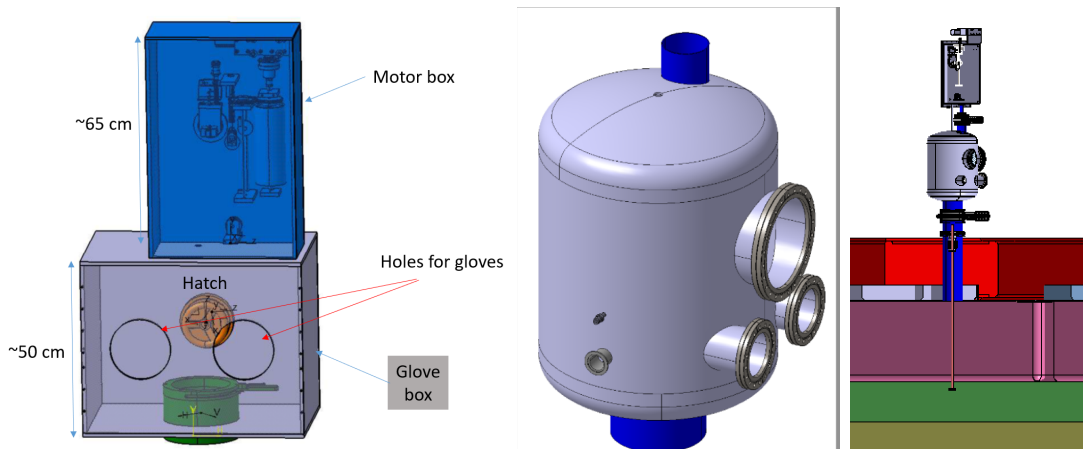


Figure 23: CAD design of a glove box seen from inside (left) and from outside (center) and integrated in the calibration system on the top of the cryostat (right).

4.2 Integration in DARKSIDE-20K

4 HARDWARE IMPLEMENTATION



Figure 24: Pictures of the glove box mock-up and its test.

614 100% Vectran LCP (Liquid Crystal Polymer) from a special clean run at Yale Cordage
615 and washed in ultrapure D₂O inside the SNO detector for years. The rope radioactivity
616 was measured at SNO. The properties at cryogenic temperature and the resistance to 100
617 N tension have been checked to be compatible with the system conditions.

618 Better discuss in this section the interfaces warm/cold and the interfaces between the
619 motor box and the glove box ? Here or elsewhere?

620 4.2 Integration in DARKSIDE-20K

621 The calibration system comprises two stainless steel pipes of almost 20 meters length
622 each. The part of each pipe located inside the cryostat would be integrated to the TPC
623 outside the main cryostat before the insertion. The different segments (typical length
624 of 3 and 6 m) forming the U up to the top cap of the cryostat would be fixed to the
625 TPC and its mechanical structure via dedicated anchors. Then, the TPC together with
626 the two pipes would be inserted in the main cryostat. The ends of each pipe would be
627 inserted in the top cap of the cryostat in each one of the four exits and then fixed to the
628 flanges. The current idea is to weld, using orbital welding, the long vertical pipes to the
629 two U-shape bottom pipes in-situ; and in addition, four sections of pipe on top of the
630 cryostat cover. The orbital welding procedure shall be assessed and practiced in 2023 on
631 tube pieces left from the mock-up.

632

633 The calibration system is implemented in the official DARKSIDE-20K CAD. The dif-
634 ferent steps for the integration are described in detail below.

- 635 1. The two pipes will cross each other below the TPC. The first step will consist in
636 installing the lower part of each pipe below the bottom optical plane (BOP). Figure
637 25 represents a view of the BOP together with these two segments of pipe. Figure
638 26 gives a similar view with the addition of the temporary support structure. The
639 pipes will be fixed to the BOP with special elements showed on Figure 27.

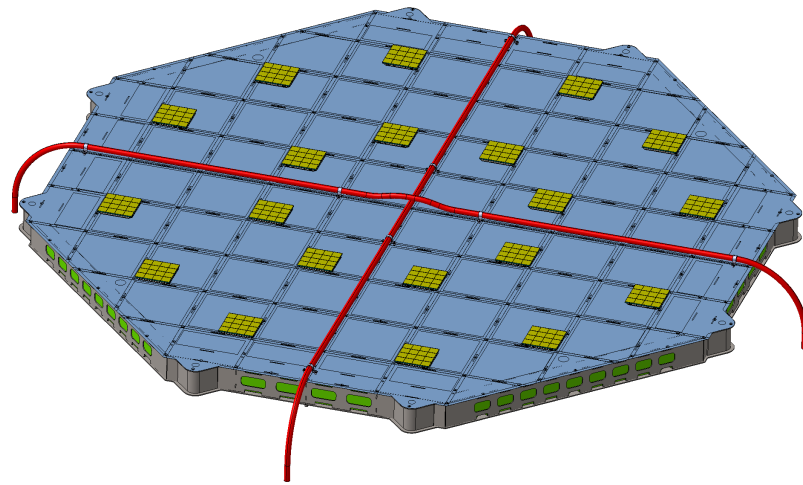


Figure 25: Calibration pipes lower sections fixed to the BOP (view from underneath the TPC).

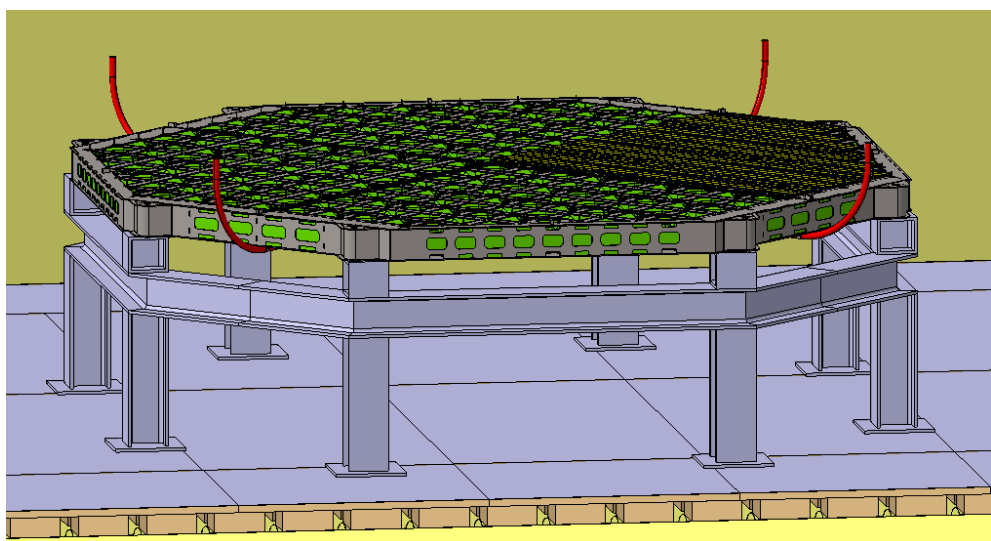


Figure 26: Calibration pipes lower sections fixed to the BOP installed on the temporary support structure.

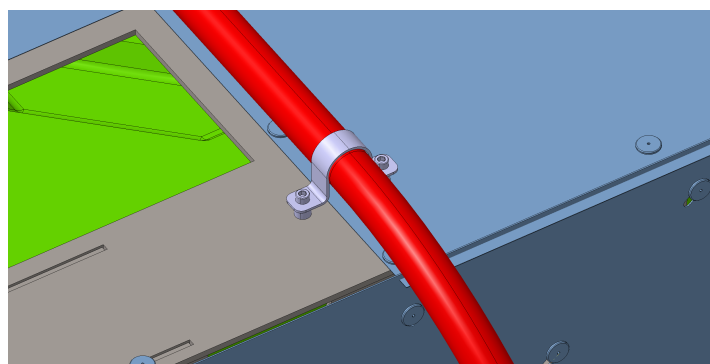


Figure 27: Detail of pipe fixation on the BOP.

- 640 2. The first two vertical sections (pink on Figure 28) of each pipe (in total, there is
 641 four vertical sections for each pipe) will then be welded. An orbital welding machine
 642 will be used to perform the welding of these segments to the lower section already
 643 installed. A straight 10 cm part is present (and highlighted on Figure 28) between
 two bent parts below and above, in order to ease the welding.

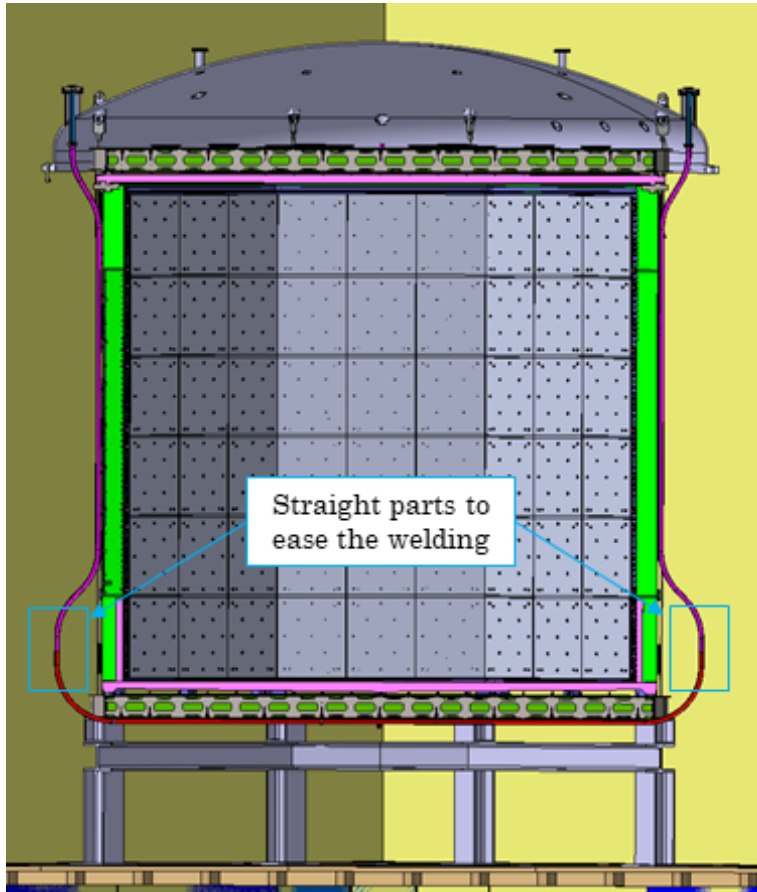


Figure 28: Side view of the inner detector with the lateral segments of the pipes integrated.

- 644
- 645 3. Two short segments (dark blue on Figure 29) will be added toward the exit of the
 646 stainless steel vessel. A flange will be used to link them to the previous segments.
 647 It is preferred over welding in case the vessel would have to be opened and the pipe
 648 dismounted. At the level of the vessel connection, we will use zero-length adapters
 649 together with flanges. Figure 29 illustrates this part of the pipe.
- 650 4. All the previous steps will take place before the insertion of the inner detector inside
 651 the stainless steel vessel. Once the insertion is done, the system will look like the
 652 view given by Figure 30.
- 653 5. Once the top cap of the cryostat is installed as well as the chimneys, the glove and
 654 motor boxes will be added as illustrated by the Figure 31.
- 655 6. The pipe sections (red) on Figures 32 and 33 coming from the glove boxes toward
 656 the inside of the cryostat will then be added.

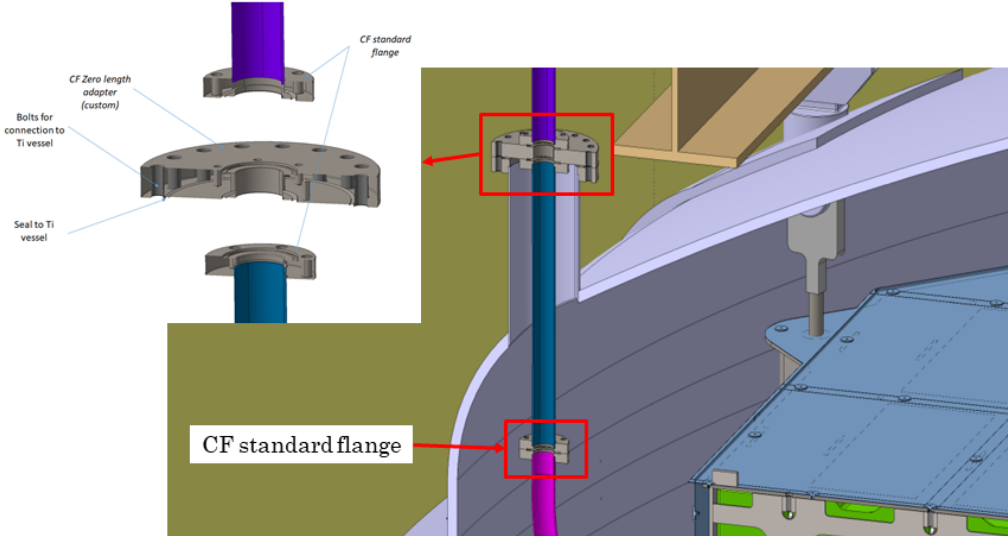


Figure 29: Sections of the pipe next to and at the level of the vessel connection.

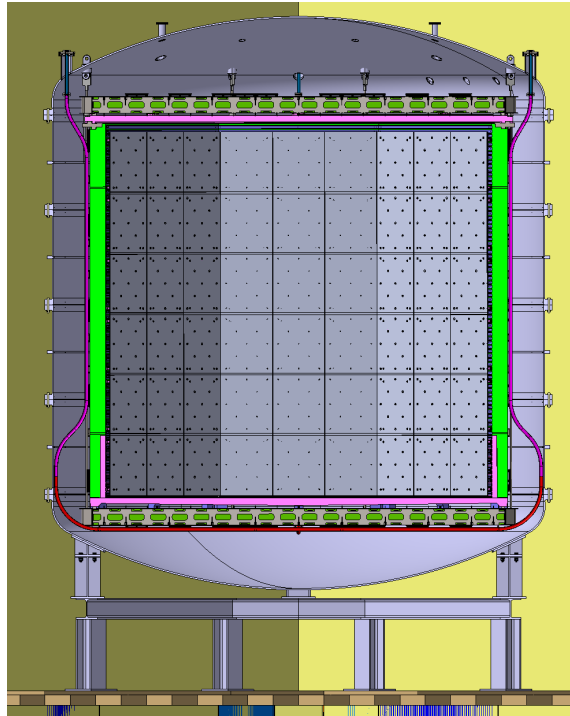


Figure 30: Lateral view after insertion of the inner detector in the vessel inside the cryostat.

- 657 7. The final step will consist in the addition of the final two sections (per pipe – purple
 658 on Figure 33) linking the top and bottom parts of the pipe. In both cases, the pipe
 659 sections are connected with flanges.

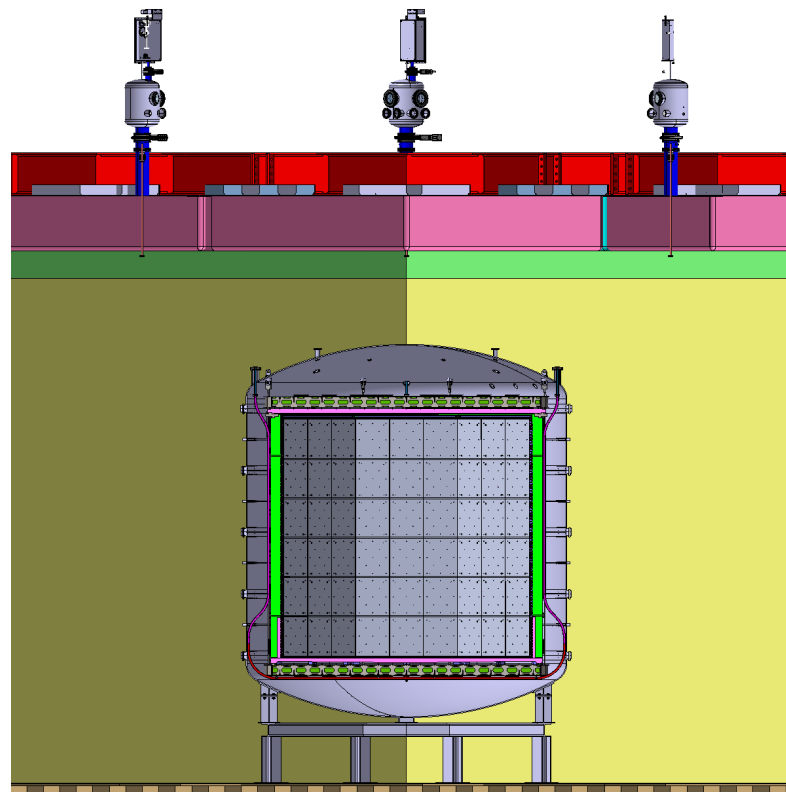


Figure 31: Lateral view after the installation of the glove and motor boxes on top of the cryostat cap.

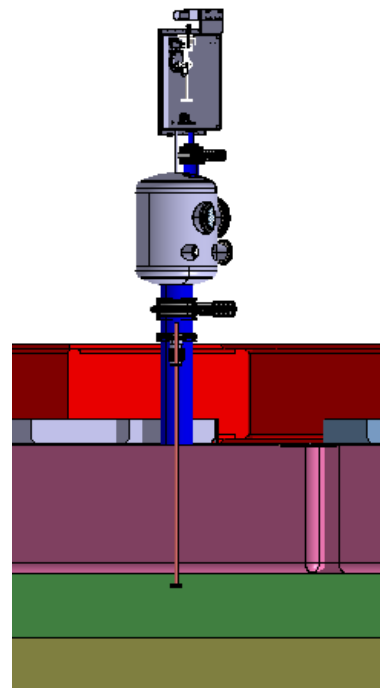


Figure 32: Lateral view of the glove and motor boxes on top of the cryostat cap with the pipe section going toward the inside of the cryostat.

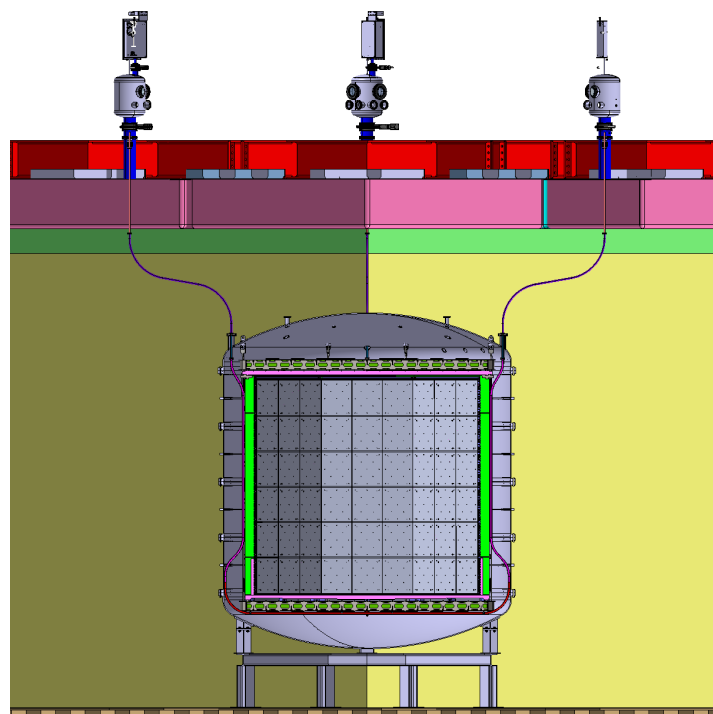


Figure 33: Lateral view after the addition of the last sections of each pipe from the vessel toward the glove boxes.

4.3 Operation in DARKSIDE-20K

661 The deployment of a rope would be done the "SNO way" by pumping out a fluffy ball,
662 with the rope attached to it, from one end of the pipe to the other. This will be tested
663 with the scale one mock-up (see section 4.4.2), together with other options of deployment.
664

665 The radio-active sources could then be inserted using the glove box following a well-
666 defined procedure illustrated in Figure 34. In short :

- 667 1. The valve is closed and a security is attached to the Rope-Calvin (Rope-C), in order
668 to prevent it dropping inside the pipe. The source is brought inside of the glove
669 box and attached to the Rope-Hobbes (Rope-H).
- 670 2. Nitrogen is flushed in the tube and the valve is opened (gaz pressure and flux to be
671 defined thanks to mock-up tests)
- 672 3. The rope-C is attached to the source
- 673 4. The security is removed
- 674 5. The run can start with the source going through the hole. The source would then
675 be moved to reach several locations (typically 6 on the side and 3 below) along the
676 pipe. At each location, calibration measurements would be performed for a duration
677 dependent of the type of source and activity. See section 3 for more details. At the
678 end, the source is back to the original position.
- 679 6. The security device is attached to the rope-C
- 680 7. The source is removed from the rope-C and put on its security device, the valve is
681 closed and the Nitrogen is not flushed anymore
- 682 8. The source is removed from rope-H and put on the shelf and then on the stocking
683 box.

684 When no source would be in use, the two ropes would be attached to anchors at their
685 extremity not linked to the motor box and the valves would be closed. The sources would
686 be stored in a dedicated locked box outside Gran Sasso (not underground).

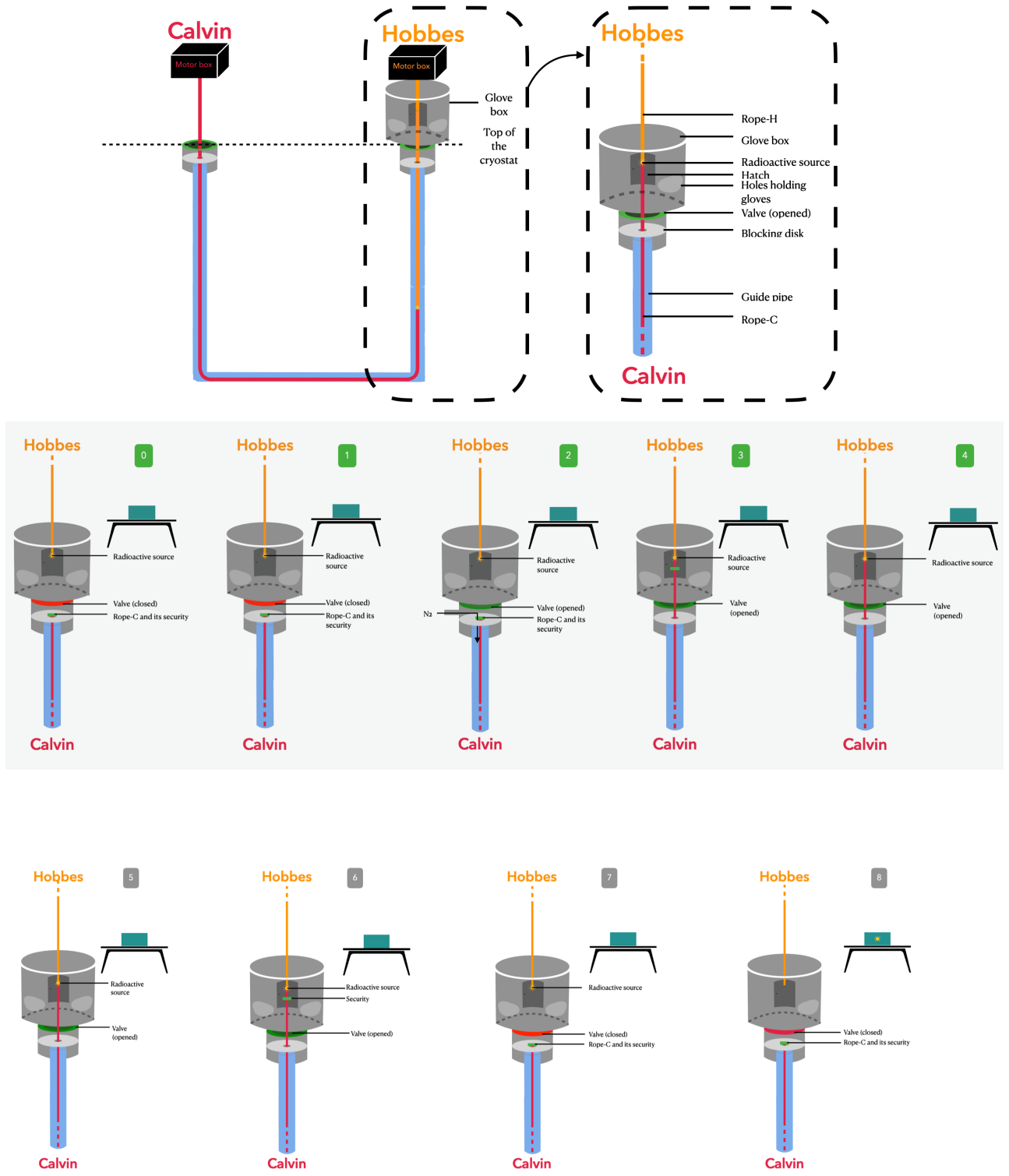


Figure 34: Procedure to be followed to attach, drive and remove the source.

687 4.4 Mock-ups

688 To validate all the choices described in section 4.1, 4.2 and 4.3 prior the running in
 689 DARKSIDE-20K, three different mock-ups have been designed. They are used to check
 690 the performance of the final system at three different levels and are described in details
 691 in this section.

692 **4.4.1 General characteristics of DARKSIDE-20K calibration system**

693 The main characteristics of the calibration system are summarized in Table 23. The
 694 goal of the system is to position the source at ± 1 cm precision, at a reasonable speed
 695 (> 1 cm/s). The tension of the rope should not exceed a value at the level of 150 N. A
 696 major problem occurs if an ice block formed into the tube and block the system : that
 697 should be avoided by the constant flush of N2 into the tube. Finally, the system should
 698 be able to smoothly drive about 10 sources back and forth per year and per pipe (the
 699 total length browser by one source is 100 m). Note that for each mock-up, a dedicated
 700 calibration of the encoders is performed to be able to run in the optimal conditions.

701 **4.4.2 Warm mock-up at scale-one (MU_W)**

702 Figure 35 left shows the scale-one mock-up whose purpose is to mimic the full-scale
 703 design with a transparent plastic tube to study the behaviour of the source and the rope in
 704 the 15 bends of the tube. Each bends reproduces the situation in the DARKSIDE-20K ex-
 705 periment and only the straight lines has been reduced to fit in the experimental hall of
 706 CPPM. A pseudo-source of 5.5 cm length, 2.2 cm diameter and weighting about 100 g
 707 is attached to each side of the rope coming from the two motors. The mock-up and the
 708 support structure needed for the motors have been installed in October 2022 and March
 709 2023, respectively. The tests were performed in March and April 2023.

710
 711 The preliminary conclusions are summarized below :

- 712 • The rope deployment in the tube was successful but complicated by the friction in
 713 the tube.
- 714 • The tension for the motor system is illustrated in Figure 35 right. It is between 60
 715 and 90 N depending on the direction of the pseudo-source and its location inside
 716 the tube. This is well below the maximum possible tension of 150 N.
- 717 • The number of bends, the total length of the tube and the tube material (plastic)
 718 may all be responsible for the rise of the tension. To better understand the be-
 719 haviour several configuration of the mock-up has been considered (Figure 36 left).
 720 The tension measured in the three options are shown in Figure 36 right. A decrease
 721 of ~ 5 N per bends is observed.

722 Few other measurements are still to be performed and are discussed in section 4.4.4.

4 HARDWARE IMPLEMENTATION

4.4 Mock-ups

	DS-20k	MU_CS	MU_CL	MU_W
General				
Goals	NA	Cold behav.	Robustness	bends source size scale 1:1
Availability Runs	10/24 >02/26	09/22 09, 11/22, 03/23	05/23 06-07/23	02/23 03/23
Conditions				
Temperature (K)	88	77	77	290
Usage time / run	30 days	8 hours	1 month	hours
Location	GS	CPPM	CERN	CPPM
Mechanics				
Pipe Total length (m)	20	~ 4	~ 2	~15
Pipe thickness (mm)	1.5	1.65	1.5	1.5
Pipe internal Diameter (mm)	30	30	33	30
Pipe Material	SS	Ti, SS	SS	Plastic
Nb of Bends / pipe ($\phi=30\text{cm}$)	14, 15	2	1	15
Source length (cm)	TBD	3	3-7	3-7
Source diameter (cm)	TBD	1	1-2.5	1-2.5
Requirements / Performance				
Speed of the source (cm/s)	> 1	3	–	2
Position Accuracy (cm)	± 1	± 1	–	± 1
Tension (N)	< 150	25-40	–	60-90
Ice formation (block)	No	No	–	NA
Total Length for one source (m)	100	> 100	–	> 100
Total nb of back&forth / pipe	10	44	–	>6

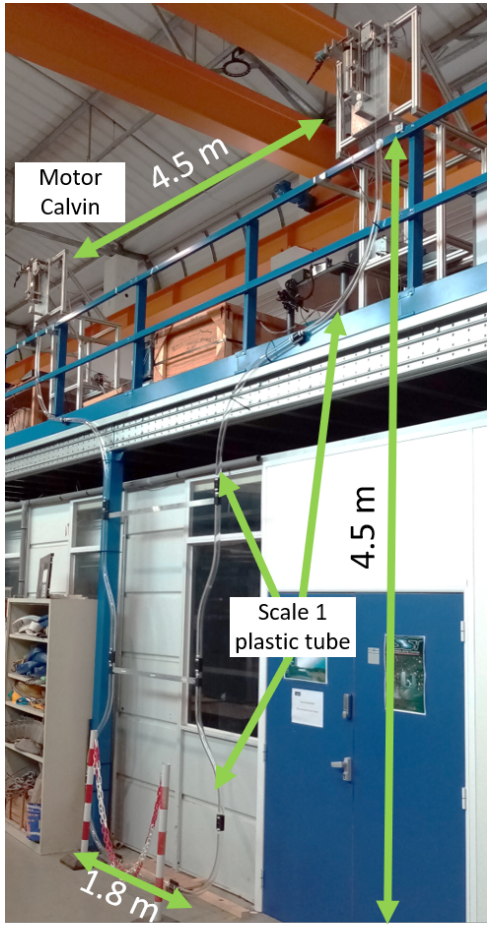
Table 23: Characteristics of the final guide pipe system and how they are addressed by the three mock-ups. Requirements from DARKSIDE-20K are put in red at the bottom. In green are the outcome of the mock-up test.

4.4.3 Cryogenic mock-up for short runs (MU_CS)

To check the behavior at liquid argon temperature of the calibration system a cryogenic mock-up has been built at CPPM and operated at liquid nitrogen temperature (77 K). It consists of a stainless steel tank ($1800 \times 90 \times 10 \text{ mm}^3$) insulated with polystyrene, and a 3 m long 30 mm diameter and 1.5 mm thickness titanium pipe ⁴. The pipe is shaped as a U and has two vertical sections of 600 mm, two curved sections with a radius of curvature of 400 mm (as foreseen for the experiment) and an horizontal section of 600 mm (Figure 37 top). The pipe is equipped with temperature sensors which are read out via National Instruments modules. Four PT100 are fixed at different location along the tube. Gaseous nitrogen is used to flush the tube and reduce the humidity to few % which is measured by a sensor, located close to the tube entrance in the cryostat. Since May 2022, the mock-up is equipped at each extremity of the pipes with the final version of the motor system and its monitoring (see Figure 37 bottom). On top of the original

⁴The pipe was ordered when DARKSIDE-20K was envisaging to have a titanium vessel.

4.4 Mock-ups



4 HARDWARE IMPLEMENTATION

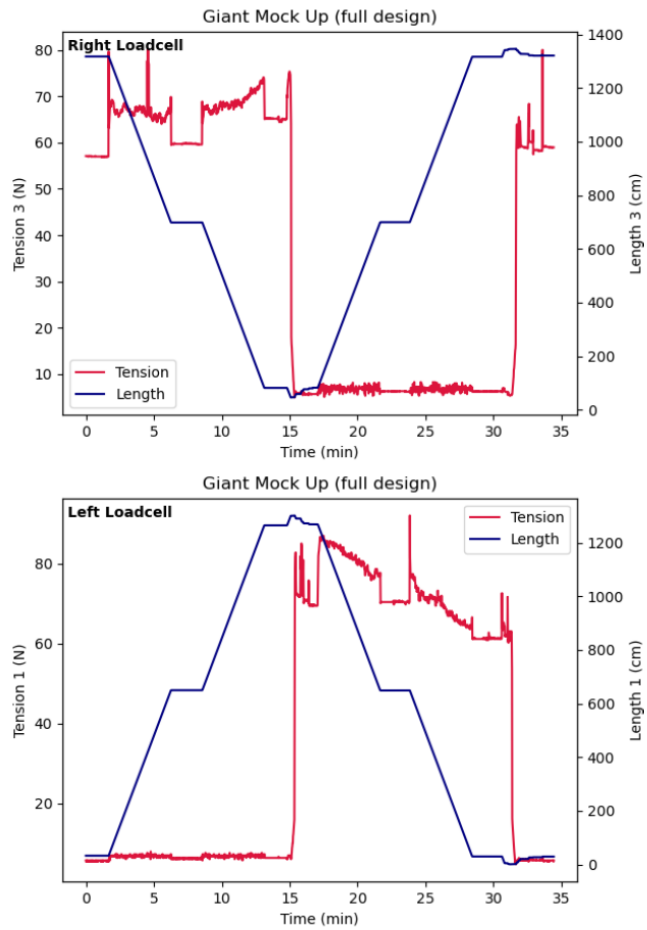


Figure 35: Left: Scale-one mock-up installed at CPPM. Right: Tension of the motor system as measured from the right (top right) and left (bottom right) loadcells along the course of the pseudo-source. The right scale shows the length in cm.

736 motor monitoring, a python software was developed to visualize the source position online.

737

738 A first run with liquid nitrogen took place in July 2021 (150 liter of LN₂ is needed),
 739 with the aim to check all the procedures involving LN₂ and measuring temperature, de-
 740 formation and humidity. Nitrogen gas was flushed inside the pipe only for a fraction of
 741 the time. A visual inspection at the end of test, accomplished by introducing a small
 742 endoscopic camera in the pipe, revealed the probable presence of small ice blocks. Fig-
 743 ure 39 top shows the temperature monitoring of the 4 probes during the test. This first
 744 test confirms that the mock-up is suited for few hours of operation at 77 K in the bottom
 745 part of the cryostat.

746

747 After the installation of the motors and of the monitoring system in the first half of
 748 2022, the set-up was completed. Warm test were carried to measure the position accu-
 749 racy using a magnet-diode system to localize the pseudo source attached to the rope. A
 750 position accuracy of ± 1 cm was measured in agreement with the DARKSIDE-20K re-

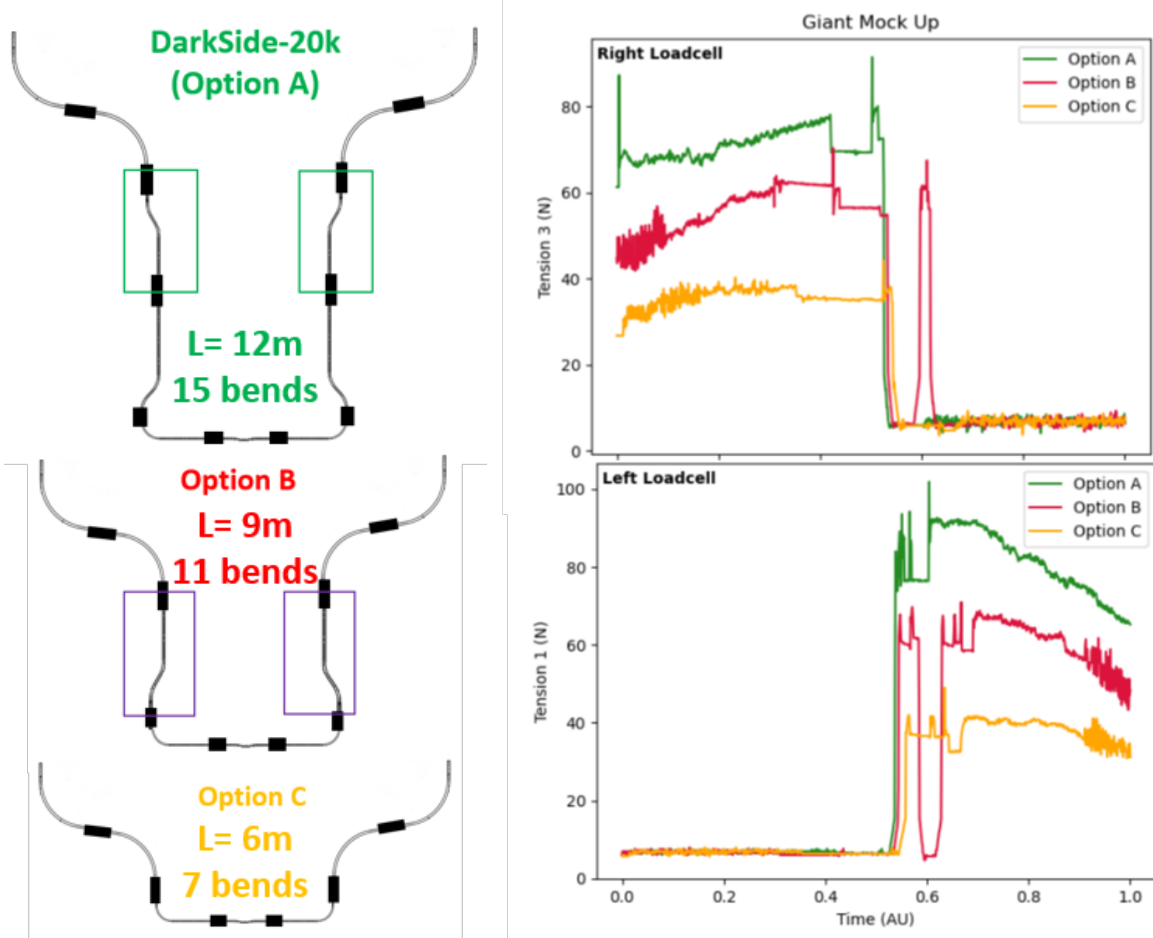


Figure 36: Left: Scale-one mock-up installed at CPPM. Right: Tension of the motor system as measured from the right (top right) and left (bottom right) loadcells along the course of the pseudo-source.

751 requirements. A typical circulation speed of 3 cm/s was also measured, satisfying the
 752 DARKSIDE-20K requirements. Finally a tension of 25-30 N was measured.

753

754 In September 2022, a first cold run test of 8 hours was carried out at cold. For this
 755 test, the pipe was flushed and kept under nitrogen gas permanently⁵. No change of
 756 behaviour of the rope between room and 77 K temperature was observed. However, the
 757 rope tension shows a slow increase with time and at some point surpassed the shutdown
 758 tension of 40 N. At the end of the run, a flexible shaft coupling broke. The reason for
 759 that is not fully clear, but could be linked to the increase of tension observed. In total
 760 during this run, 70 round trips were done corresponding to 210 m which is above what
 761 is envisaged for one source in DARKSIDE-20K.

762

763 Second and third run were conducted in November 2022 and March 2023. For these

⁵At the end, the flushing was stopped to see if this favors the formation of ice blocks. An endoscope camera inspection was performed and noticed two small ice block formation.

4.4 Mock-ups

4 HARDWARE IMPLEMENTATION

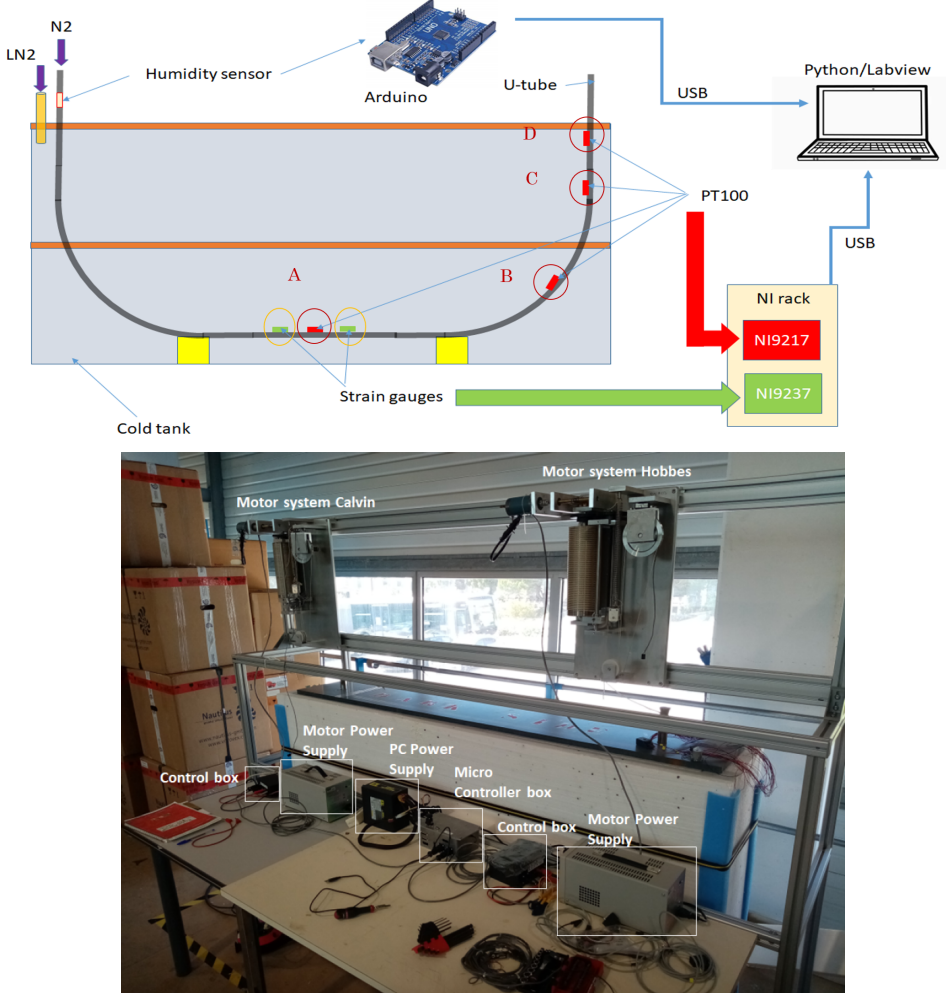


Figure 37: Top: Simple schematic of the cryogenic mock-up build at CPPM. Bottom: Picture of the fully integrated system with the two motors including the power supply and the controller (the monitoring PC is not shown on this picture).

764 runs, both flexible shaft couplings were replaced. This time the N2 flushing was constant.
 765 The tension needed to pull the source was similar to the September run with a tension
 766 never exceeding 40 N – except when the circulation is stopped for few minutes where the
 767 restart tension can raise up to 50 N. Figure 39 bottom shows the variation of the tension
 768 measured during the run. For each run, >40 round trips were done corresponding to
 769 100 m. No problem was observed on the flexible shaft. At the end of the last run an
 770 endoscope camera was used for inspection of the tube when the temperature was -23 C
 771 at the bottom of the tube. Very thin layer of frost observed but no ice block formation.
 772 Figure 38 shows two pictures of what was observed by the camera.

773

774 The conclusions of the tests with respect to the requirements of DARKSIDE-20K ex-
 775 periment are summarized in Table 23.

776



Figure 38: Picture taken by the endoscopic camera inside the tube after the cold test.

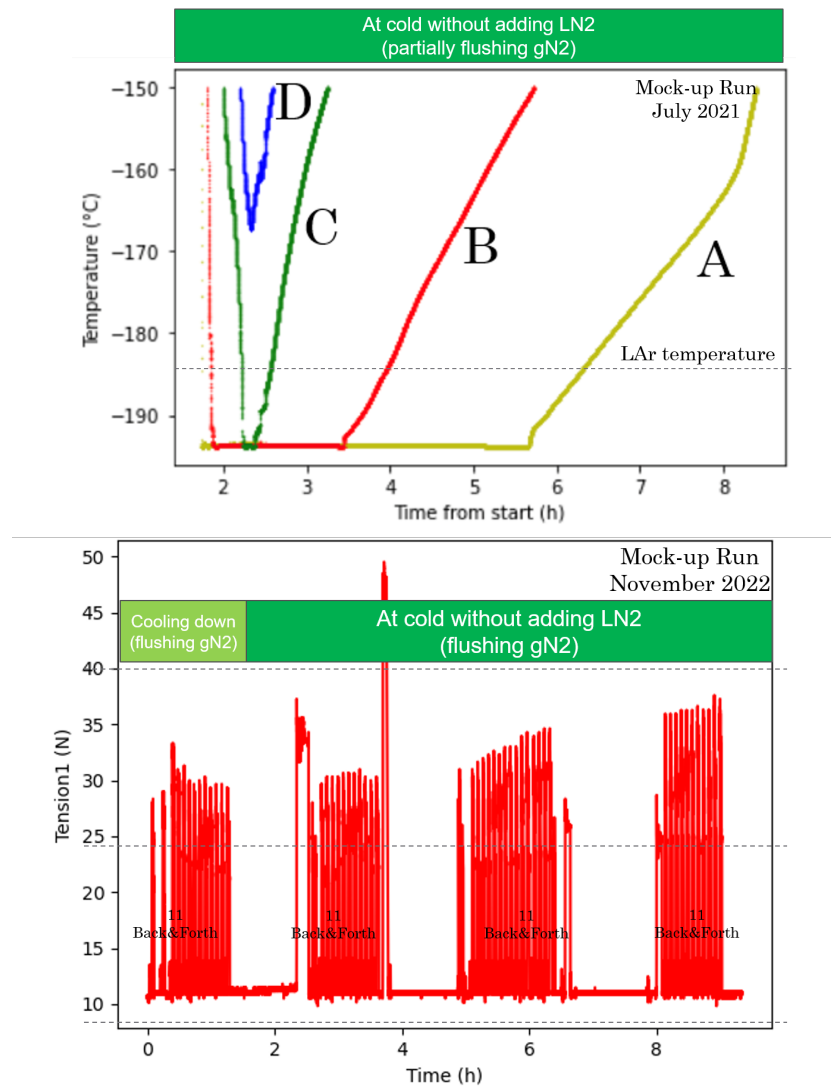


Figure 39: Top: Temperature probe measurements during the first cold test after the cooling down completed (July 2021). The letters A, B, C, D corresponds to PT100 probes of Figure 37 and the Liquid argon temperature is indicated. Bottom: Tension measured during the third run (November 2022).

777 4.4.4 Remaining tests at CPPM

778 Two remaining tests are foreseen before the summer break in order to :

- 779
- 780 • Compare the tension of the material (plastic, SS and Titanium) at warm on a simple
4 meter, two-bends tube. Conclude on the impact of the material on the friction.
 - 781 • Establish a procedure to remove ice blocks already formed in the tube. Due to
782 the short time available at cold with MU_CS (8 hours), it was not convenient to
783 perform this test. It was decided to insert an ice block in a bend segment immersed
784 in LN2 and flush gN2 in it to see whether the block can be eliminated.

785 **4.4.5 Cryogenic mock-up for long runs (MU_CL)**

786 As just mentioned, longer periods are needed to test the robustness of the calibration
787 system and proceed to a typical DARKSIDE-20K run as described in Table 6 and 8. The
788 CERN cryolab team offered the possibility to do first tests in June 2023 with a cryostat
789 shown in Figure 40 right. The test should last typical one month to be representative of
790 the situation in DARKSIDE-20K. This will also allow to evaluate if the rope can break :
791 this will be done by running the source 10 times (or some other safety factor) the length
792 expected during all of DS-20k calibration (see section 4.4.5). The two motors, with the
793 final design as the ones used at CPPM, will be installed on support structures at CERN.
794 Tests will be conducted at liquid nitrogen temperature for one month. An illustration of
795 the set-up is shown in Figure 40 left.

796 With this mock-up, it will also be possible to study the impact of the source size and
797 weight on the tension of the motor system. For this several 3D-printed elements (2.5, 2.7
798 and 29 mm in diameter and from **3 to 7 cm in length** have been manufactured at CPPM,
799 see Figure 41).

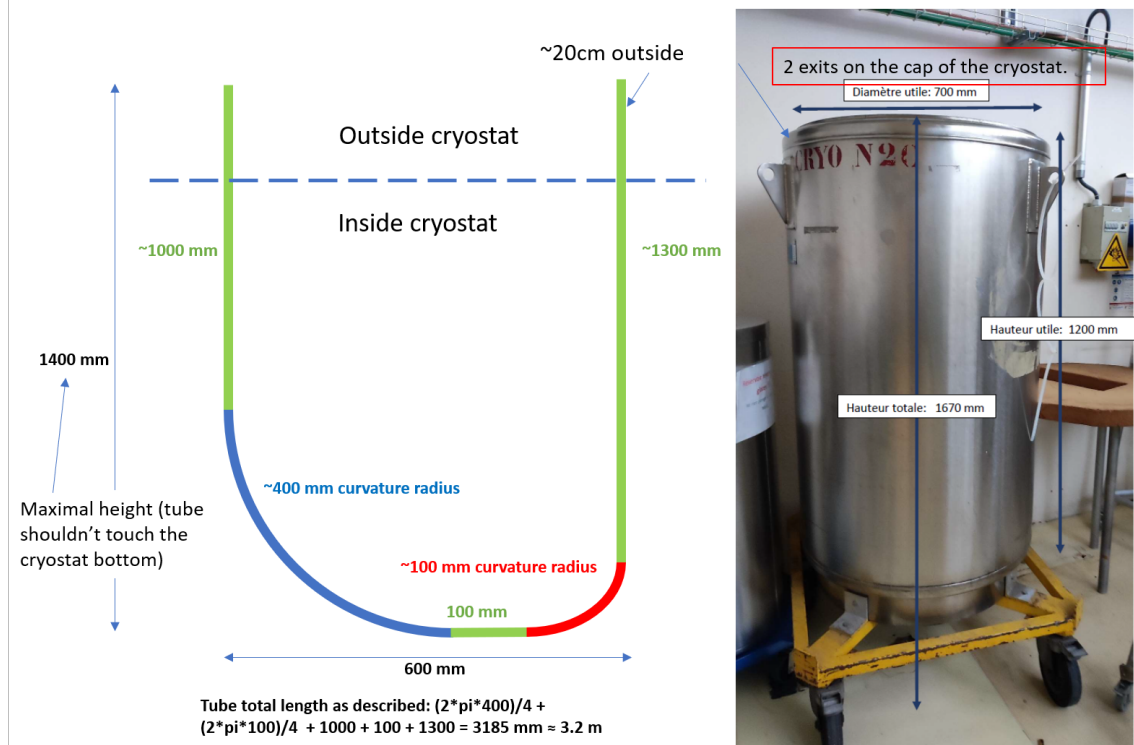


Figure 40: Left: Mock-up to be operated at CERN for long term measurements. Right: Cryostat to be used for the CERN tests.

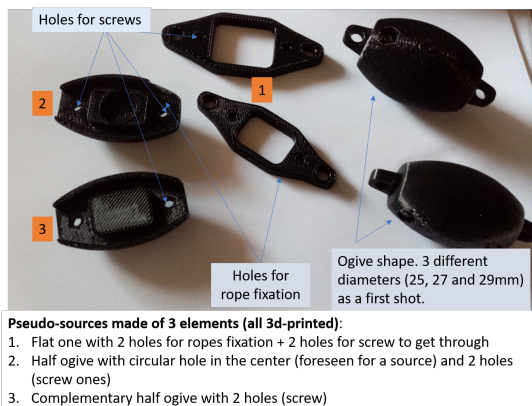


Figure 41: Pseudo-sources to be tested in the mock-up.

5 Conclusions

In this note the design of the DARKSIDE-20K calibration pipe system (as of January 2023) is summarized. It is included in the DARKSIDE-20K simulation package and a tentative calibration program has been elaborated. The background brought by the system is negligible and the light yield reduction in the veto system mitigated by the coating of the pipe.

The hardware implementation in DARKSIDE-20K is finalized. Two of the three mock-up, needed to validate this design, are constructed and few hours of smooth running of the system at cryogenic temperature was possible in November 2022. In 2023, the mock-up program will be continued and completed, allowing to reach the final conclusions for the calibration system in DARKSIDE-20K at the end of Summer 2023.

811 **Acknowledgements**

812 We would like to thank Hanguo Wang for the many discussions and advices when
813 designing the guide pipe system and when writing this document.

814 **References**

- 815 [1] DarkSide Collaboration. *DarkSide-20k Technical Design Report*. 2021, docdb-4637.
- 816 [2] DEAP-3600 Collaboration. *First results from the DEAP-3600 dark matter search*
817 *with argon at SNOLAB*. *Phys. Rev. Lett.*, 121(7):071801, 2018, arXiv:1707.08042.
- 818 [3] DEAP-3600 Collaboration. *Search for dark matter with a 231-day exposure of*
819 *liquid argon using DEAP-3600 at SNOLAB*. *Phys. Rev. D*, 100:022004, 2019,
820 arXiv:1902.04048.
- 821 [4] DarkSide Collaboration. *Low-Mass Dark Matter Search with the DarkSide-50 Ex-*
822 *periment*. *Phys. Rev. Lett.*, 121:081307, 2018, arXiv:1802.06994.
- 823 [5] DarkSide Collaboration. *Calibration of the liquid argon ionisation response to low*
824 *energy electronic and nuclear recoils DarkSide-50*. *Phys. Rev. D*, 104:082005, 2021,
825 arXiv:2107.08087.
- 826 [6] European Strategy for Particle Physics Preparatory Group. ‘*Physics Briefing Book*’.
827 arXiv:1910.11775.
- 828 [7] Cooley, Jodi. *Dark Matter Direct Detection of Classical WIMPs*. arXiv:2110.02359.
- 829 [8] P. Agnes et al. CALIS—A CaLibration Insertion System for the DarkSide-50 dark
830 matter search experiment. *JINST*, 12(12):T12004, 2017, 1611.02750.
- 831 [9] DarkSide Collaboration. *Source list from DS50*. 2014, docdb-938-v7.
- 832 [10] DarkSide Collaboration. *AmC source for DS50*. 2016, docdb-1498.
- 833 [11] DarkSide Collaboration. *AmBe source for DS50*. 2016, docdb-1516-v3.

834 A Sources

835 Table 24 shows the diameter, length and activity of the various sources taken from
 836 DS-50 [8]. The source capsule was a leak-tight cylinder of 31 mm outer diameter [9]
 837 and 65 mm length [9]. The gamma source itself is a 1" plastic disk of 2-3 mm thickness.
 838 The AmC source [10] used in DS-50 gives 1 n/s composite neutron source was about a
 839 cylinder 28 mm in diameter and 19 mm in thickness. There was no dimension constraints
 840 in DS-50 for the source capsule, so this could have been smaller.

841

Sources	Photons				Neutrons	
	^{57}Co	^{133}Ba	^{22}Na	^{137}Cs	AmBe	AmC
Source holder						
Diameter (cm)	1	2.5	2.2	0.4	0.5 (1.5)	2.78
Length (cm)	0.2	0.3	0.3	0.4	1.5 (5)	1.92
Activity (kBq)	35	2.0, 3.8	11	0.65	0.01 (2)	0.001
Source Capsule						
Diameter (cm)	3.1	3.1	3.1	3.1	1.8 (3.1)	3.1
Length (cm)	6.5	6.5	6.5	6.5	5.2 (6.5)	6.5

Table 24: Diameter, size and activity of the source capsules used by the calibration system of DS-50 [8, 9, 10, 11]. 1 kBq corresponds to 1000 n/s

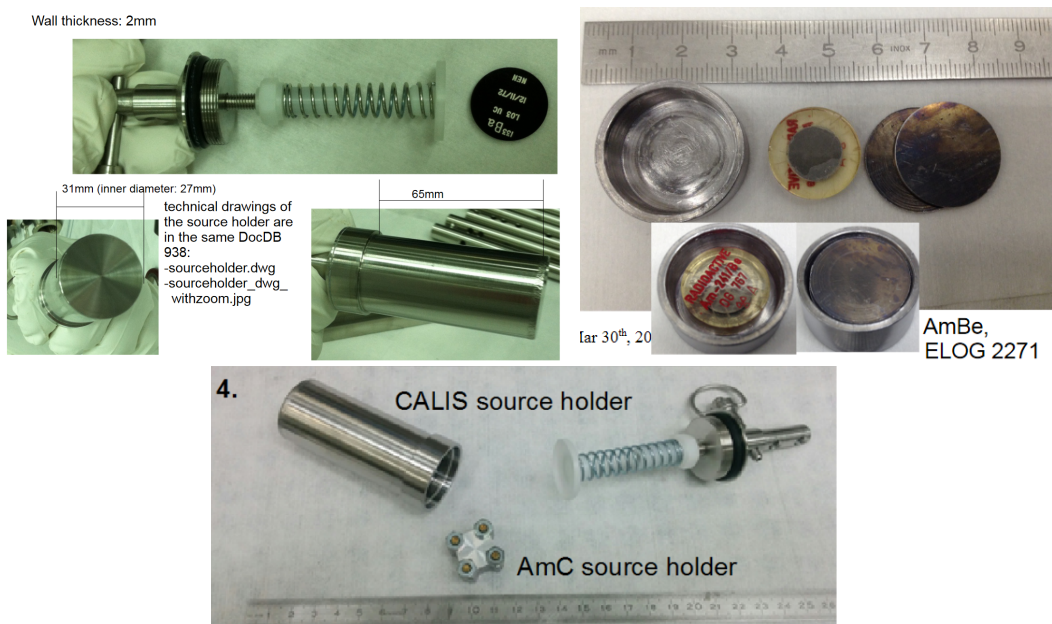


Figure 42: Photo of the DS50 source capsule for photon [9] (top left), for the AmBe source (top right) [11] and for the AmC source (bottom) [10].

842 Information from other experiments:

- 843 • AmC source from Daya Bay was roughly 10 mm in diameter and 5 mm in thickness
 844 with below 1Hz neutron activity.

A SOURCES

-
- 845 ● Borexino utilized 25 mm diameter spherical quartz vial and another source holder
846 that was 35 mm long and 10 mm in diameter.
- 847 ● their AmBe source had a 3 mm Pb shield and a thick (25 mm?) delrin shield around
848 it.

849 For DARKSIDE-20K, we will need at least **3-5 mm** clearance around the source capsule,
850 so usable diameter is less than **20-24 mm** in a 30 mm diameter tube. First attempts for
851 DARKSIDE-20K are presented in Table 25. The size of the available DD gun presently
852 prevents its usage in the calibration system. For DARKSIDE-20K we need to make 60-100
853 n/s AmC source.

Sources	Photons					Neutrons				DD
	^{57}Co	^{133}Ba	^{22}Na	^{137}Cs	^{60}Co	AmBe	AmC	AmLi		
Source										
Diameter (cm)	?	?	?	?	?	?	?	?	?	
Length (cm)	?	?	?	?	?	?	?	?	?	
Activity (kBq)	100	5.0	0.67	4.6	0.6	0.2	0.2	?	0.2	
Source Capsule										
Diameter (cm)	$<2.4?$							4.4 (3.8)		
Length (cm)	$<5?$							13.0 (10)		

Table 25: Diameter, size and activity of the sources to be used by the calibration system of DARKSIDE-20K. The activities are taken from section 3.

854 B GANTT

855 Figure 43 and 44 show the current status of the GANTT_P6 and GANTT as of 4-Jan
 856 2023. Need update to include CERN cold test at least.

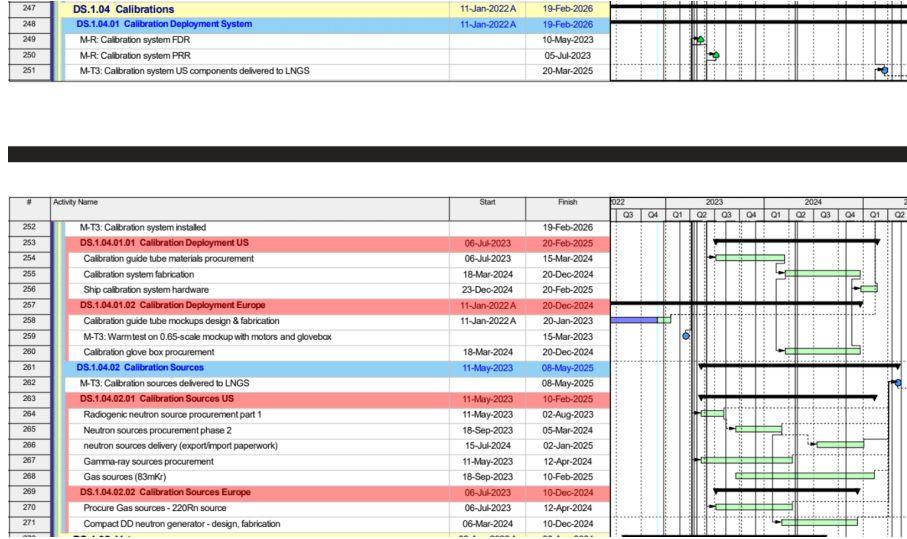


Figure 43: GANTT P6 on calibration activities as of Jan 2023.

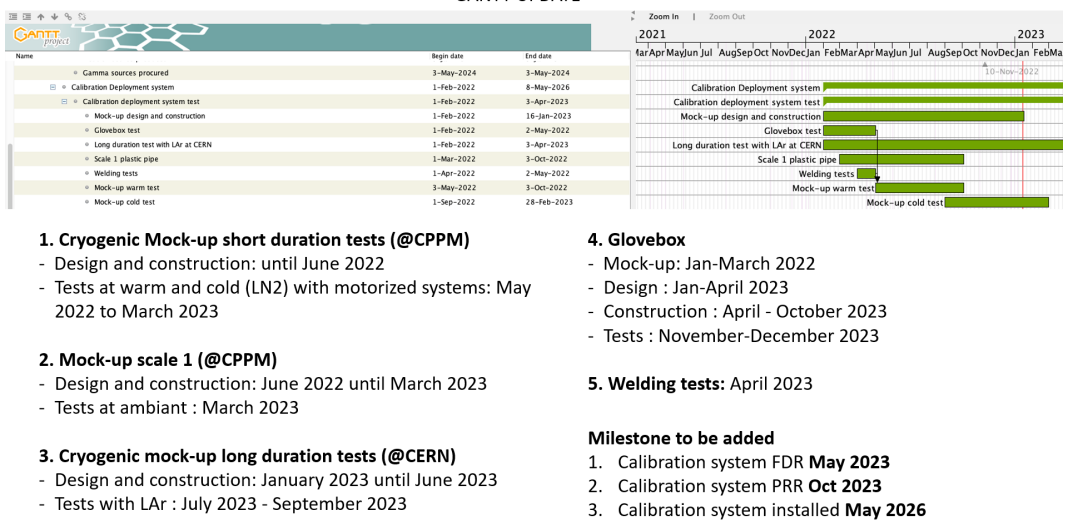


Figure 44: GANTT on calibration activities as of Jan 2023 with updates proposed below

C COSTBOOK AND BASIS OF ESTIMATE (BOE)

C Costbook and Basis of Estimate (BoE)

Figure 45 shows the current status of the costbook as of Jan 2023. Three agencies are participating : IN2P3 (France), NSF (US) and NCNP (Poland). The former concentrate on the calibration system, the latter on the ^{220}Rn source and NSF participate to both. The NSF funds All the funds mentionned in Figure 45 are already available. The total gives 325 k€ for equipment and 100k€ for labor (NSF).

863

Sum of GL Tot [EU]	Column Lat	AEI	CAS	CFI	DOE	FNP	IN2P3	INFN	NSF	NCNP	SNSF Russia	Brasil	Grand Total	
Row Labels														
= D5.0 Management Coordination					€2'258'626			€2'103'500	€527'688				€4'889'814	
D5.0.01 Management Support					€2'258'626			€2'103'500	€527'688				€4'889'814	
= D5.1 Detector		€874'250	€608'959	€8'034'967			€150'000	€220'000	€2'268'000	€8'528'450	€35'000	€22'500	€213'885	#####
DS.1.01 UAr Cryogenics					€66'033			€121'000	€2'365'980				€2'553'013	
DS.1.02 Inner Detector		€83'000	€547'400	€4'721'597				€719'000	€5'740'052				#####	
DS.1.03 Materials		€756'250						€130'000	€57'036	€25'000			€968'286	
DS.1.04 Calibrations							€50'000		€365'382	€10'000			€425'382	

Figure 45: CostBook status as of Jan 2023.

The amount expected or already spent for the calibration system and sources is shown in Table 26. The estimated cost is approximately split half-half in between the calibration system and the sources. The cost is well within budget with a margin of 140 k€.

k€	Calibration System (IN2P3, NSF)					Sources (NCNP, NSF)				Total
	Mock Up	Guide Tubes	Motors boxes	Glove boxes	Ropes	γ	n	Gas	^{83m}Kr	^{220}Rn
Est. Cost	25	10	10	80	1	70	46	24	10	276
Spent	22	0	6	0	1	0	0	0	0	29
To be spent	3	10	4	80	0	70	46	24	10	247

Table 26: Costs in k€ for each component of the calibration system and sources as of Jan-2023. No labor cost is included. Gas refers to ^{83m}Kr and ^{220}Rn injected in the liquid argon system.

Figure 46 shows the basis of estimates for the various sources and Figure 47 shows the basis of estimates for system deployment. A summary is shown in Figure 48

C COSTBOOK AND BASIS OF ESTIMATE (BOE)

• **Basis of Estimate:** The estimate is based on quotation from Eckert & Ziegler dating Dec 2020, including sources and estimated shipping cost listed therein. The cost is: \$19,160 for 8 capsules ^{137}Cs (\$2,395/each per quote above); \$19,880 for 8 capsules of ^{57}Co (\$2,485/each per quote above); \$22,600 for 8 capsules of ^{60}Co (\$2,825/each per quote above). Gamma-rays source will be consolidated for shipment by source type. Shipping and packaging for each source type is estimated to be about \$4,000 based on prior experience with the DarkSide-50 experiment, for a total of \$12,000 for the three source types. The gamma-ray sources set is a significant equipment item that can be inserted in the customs exempt list of items in the underground LNGS and is not subject to customs duties;

- **Fully Burdened Cost:** \$73,640;
- **Funding Profile:** \$14,720/\$29,460/\$29,460 (YR1/YR2/YR3);
- **Project Cost Category:** Non labor;

- **NSF Budget Category:** Equipment.

• **Basis of Estimate:** The estimate for the $^{241}\text{Am}^{13}\text{C}$ sources is based on quotation "Hawaii Quote 1.04.02.50 Eckert & Ziegler", including sources and estimated shipping cost listed therein. Fabrication of the four $^{241}\text{Am}^{13}\text{C}$ sources comes at a cost of \$18,620 (\$4,255/each for ^{241}Am per quote above, and \$400/[gr ^{13}C] for 1 gr of ^{13}C required for each source, based on the website catalog cost of possible suppliers (Sigma Aldrich website), for a total of \$4,655/each for the four $^{241}\text{Am}^{13}\text{C}$ sources). The estimate for the four $^{241}\text{AmBe}$ is of \$17,840 (\$4,460/each, based on prior experience with the procurement of similar sources for the DarkSide-50 experiment and for own laboratories). Finally, one $^{241}\text{AmLi}$ source will be fabricated in-house at total cost of \$4,317 (\$4,255 for ^{241}Am per quote above, and \$62/[100 gr LiOH] for the 100 gr LiOH required, based on the website catalog cost of possible suppliers (Sigma Aldrich website)). AmC and AmLi source capsules will be shipped together as they are both custom made, while AmBe source capsules will be shipped in a second, separate second batch. Shipping and packaging for each source shipment is estimated to be about \$4,000 based on prior experience with the DarkSide-50 experiment, for a total of \$8,000 for the two expected shipments. The neutron source set is a significant equipment item that can be inserted in the customs exempt list of items in the underground LNGS and is not subject to customs duties;

- **Fully Burdened Cost:** \$48,777;
- **Funding Profile:** \$20,100/\$16,126/\$12,551 (FY21/FY22/FY23);
- **Project Cost Category:** Non labor;
- **NSF Budget Category:** Fabrication.

• **Basis of Estimate:** The estimate is based on quotation from National Isotope Development center and dated January 2021. It details the cost of \$620 for the production of the ^{83}Rb batch and of \$5150 for a radioisotope dispensing/packaging fee, for a total of \$5770. Our basis of estimate includes provision for a total of two batches amounting to \$11540. It also includes provision for shipping costs, estimated base on prior experience at \$1000 per shipment, for a total of \$2000, and a cost of construction of the source holder and dispenser, estimated on the basis of prior experience at \$730 per unit, for a total of \$1460.

- **Fully Burdened Cost:** \$15,000;
- **Funding Profile:** \$0/\$7,500/\$7,500 (YR1/YR2/YR3);
- **Project Cost Category:** Non labor;
- **NSF Budget Category:** Equipment.

Figure 46: Base of estimate for gamma (top), neutron (center) and Krypton (bottom) sources.

C COSTBOOK AND BASIS OF ESTIMATE (BOE)

BoE for Activity 1.04.01.10
"Calibrations system engineering support"
[Calibrations, DS-20k]

Institution: University of Hawaii;
Responsible Manager: Jelena Maricic;
Description: Funds are requested for engineering support at Hawaii. Engineering effort will be front-loaded in the first two years. The engineer will be involved in the design and construction of the guide system for deployment of small sources in the TPC and veto, and in the design and construction of the deployment system to accommodate D-D neutron generator. The Department of Physics at University of Hawaii has a well-equipped shop with CNC capabilities and two technicians are supported full time by the university. The PI intends to use their services for all standard part fabrication, and no budget for the technician time is necessary. Additional resources for the fabrication effort will come from the IN2P3 group of CPPM in Marseille, France;
Basis of Estimate: The estimate is based on the standard hourly rate at the University of Hawaii, with application of fringe and overhead in addition. We estimate the need for 4 months/year of support for each of Yr1 and Yr2. A 3% salary increase is applied for Yr2.
Fully Burdened Cost: \$98,174;
Funding Profile: \$48,361/\$49,813/\$0 (FY21/FY22/FY23);
Project Cost Category: Labor;
NSF Budget Category: Labor.

BoE for Activities 1.04.02.10, 1.04.02.30, 1.04.02.35, 1.04.02.40
"Calibrations deployment system"
[Calibrations, DS-20k]

Institution: University of Hawaii;
Responsible Manager: Jelena Maricic
Description: The TPC and veto guide tube system, or calibrations deployment system, will include 8 deployment ports, 4 for the TPC and 4 for the veto. Each deployment port consists of U-shaped pipes surrounding the detector elements of interest, equipped with stepper motors on each side to move the cable with attached source back and forth and maintain tension at all times. The calibration ports will also be equipped with gloveboxes on one side of the U-shaped pipes. The calibrations deployment system will require some special adapters to accommodate the miniature D-D neutron generator under fabrication by the BNRU group in Russia and associated power supply: the D-D-generator requires constant high voltage supply during deployment, thus cannot simply be deployed like other calibration sources. The adapters include: a HV feedthrough; a cryogenic high voltage cable; a pulley to control HV cable slack; a D-D generator deployment cable interface; a high voltage power supply and miscellaneous small parts;
Basis of Estimate: The estimate includes the cost of components, with major cost drivers supported by a quotation or website catalog quotation, and the rest, supported by prices obtained from website catalogs, listed in the table below. The glovebox cost of \$19,683/each is supported by website catalog quotation "Hawaii Quote 1.04.02.30 Terra Universal", for a total cost of \$78,732 for the 4 gloveboxes; the cost for motor drives of \$5,652/each is based on quotation "Hawaii Quote 1.04.02.30 Tekmatic", resulting in a total cost of \$22,608 for the 4 drives; 4 power supplies will be procured at cost of \$490/each, for a total cost of \$1,960; the table below also lists all other necessary small equipment items, with cost estimates supported by website catalog prices. The cost of the adapter for the D-D neutron generator is estimated, on the basis of prior experience and web catalog prices, at \$5,000 (\$533 for HV cable, \$557 for HV feedthrough, \$1,335 for HV power supply, \$1,500 for HV cable pulley fabrication, \$600 for D-D generator deployment cable interface, and \$475 for miscellaneous small parts), for a total of \$20,000 for the set of 4 adapters. The calibrations deployment system is a significant equipment item that can be inserted in the customs exempt list of items in the underground LNGS and is not subject to customs duties;
Fully Burdened Cost: \$148,780;
Funding Profile: \$94,084/\$54,696/\$0 (FY21/FY22/FY23);
Project Cost Category: Non labor;
NSF Budget Category: Fabrication.

Figure 47: Base of estimate for calibration system deployment and labor.

C COSTBOOK AND BASIS OF ESTIMATE (BOE)

Basis of Estimate
Institution: University of Hawaii
Principal Investigator: Jelena Maricic

The following table presents the requested budget summary and the budget profile of the WBS items under the responsibility of the Hawaii group.

WBS Item and Number	FY2021	FY2022	FY2023	Total
TPC and veto deployment sys. eng. support (L) WBS 1.04.01.10	\$48,361	\$49,813	\$0	\$98,174
TPC and veto deployment system fabrication WBS 1.04.02.10, 1.04.02.30, 1.04.02.35, 1.04.02.40	\$94,084	\$54,696	\$0	\$148,780
Radiogenic neutron sources WBS 1.04.02.50	\$20,100	\$16,126	\$12,551	\$48,777
Gamma Ray Sources WBS 1.04.02.65	\$14,720	\$29,460	\$29,460	\$73,640
Gas Sources 83mKr WBS 1.04.02.70	\$0	\$7,500	\$7,500	\$15,000
Total	\$177,265	\$157,595	\$49,511	\$384,371

Figure 48: Summary of the Base of estimate.

869 **D RISKS**
D Risks

870 Figure 49, 50, 51 and 52 shows the risk assessments for the guide tube system. Fig-
871 ures 53, 54, 55 and 56 shows the risk assessments for the sources.

Risk ID	<i>The Risk Manager assigns this</i>		
Submitter	Isabelle Wingerter-Seez	Risk Owner	Jelena Maricic, Pierre Barrillon
Date	2021.11.16	Risk Short Title	Ice
Risk Time Frame	From day 1 to the end of the experiment		
Earliest Impact Date	From the day the titanium vessel is filled	Latest Impact date	End of the experiment

Risk Long Title: Ice formation inside the calibration pipe.										
Risk Description: The calibration pipes will be first flushed with N2 gas and then kept under pressure with N2 gas, to remove humidity and then preserve the humidity free atmosphere. In case of a wrong manipulation, air could enter the pipe and ice be formed, on the long term.										
Detailed Risk Cause: Wrong manipulation (air leaks inside) or improper strategy of operation.										
Detailed Risk Effect: Major/Compromised performance; in case an ice block would form inside the calibration pipe, the system could not be operated.										
Describe possible Mitigation Plan(s): It is planned to keep the pipe under pressure with N2 gas during physics data taking; and flush N2 gas during calibration runs. In order to define a procedure where this risk is eliminated, tests are being carried out with a mockup, involving LN2. Further long term testing (~six months) is being considered inside the prototype ProtoOne. Ways to possibly melt the ice w/o emptying the vessel will also be studied.										
WBS Affected: <i>use the WBS name here. Risk Mgr may fill in the WBS number</i>										
<table border="1"> <thead> <tr> <th>Probability, as %</th> <th>Cost Impact, in currency and value</th> <th>Schedule Impact in working Days</th> <th>Technical Impact</th> <th>Safety/Environment Impact</th> </tr> </thead> <tbody> <tr> <td>% ?????</td> <td>One year of operation ?</td> <td>One year ? (warm up)</td> <td>Compromised performance</td> <td>Acceptable</td> </tr> </tbody> </table>	Probability, as %	Cost Impact, in currency and value	Schedule Impact in working Days	Technical Impact	Safety/Environment Impact	% ?????	One year of operation ?	One year ? (warm up)	Compromised performance	Acceptable
Probability, as %	Cost Impact, in currency and value	Schedule Impact in working Days	Technical Impact	Safety/Environment Impact						
% ?????	One year of operation ?	One year ? (warm up)	Compromised performance	Acceptable						

Figure 49: Guide tube system Risk1

Risk ID	<i>The Risk Manager assigns this</i>		Risk Type	Threat
Submitter	Isabelle Wingerter-Seez		Risk Owner	Jelena Maricic, Pierre Barrillon
Date	2021.11.16		Risk Short Title	Source blocked
Risk Time Frame	From day 1 to the end of the experiment			
Earliest Impact Date	From the first day a source is introduced in the pipe	Latest Impact date	End of the experiment	

Risk Long Title: Source detached, dropped or stuck inside the calibration pipes.				
Risk Description: During operation, insertion, circulation and removal of the source, it may drop inside the pipe. The threads may break, leading to the source remaining in the pipe. The source could detach itself from the thread and remain in the pipe.				
Detailed Risk Cause: Wrong manipulation or improper strategy of operation.				
Detailed Risk Effect: Severe; the source would illuminate the detector.				
Describe possible Mitigation Plan(s): Build a robust system and investigate all possible means of wrong manipulation. The procedure to introduce and remove the source will be designed, tested and exercised in order to provide a robust system where such event could not happen. For instance, the fact that the source is attached on two locations with two independent threads drastically limits the risk of loosing the source in the pipe. A procedure to flush or push it out could be conceived.				
WBS Affected: <i>use the WBS name here. Risk Mgr may fill in the WBS number</i>				
Probability, as %	Cost Impact, in currency and value	Schedule Impact in working Days	Technical Impact	Safety/Environment Impact
% ?????	Experimental time lost	From one month to one year	Severe	Minimal

Figure 50: Guide tube system Risk2

D RISKS

Risk ID	<i>The Risk Manager assigns this</i>	Risk Type	Threat
Submitter	Isabelle Wingerter-Seez	Risk Owner	Jelena Maricic, Pierre Barrillon
Date	2021.11.16	Risk Short Title	Pipe leak
Risk Time Frame	From day 1 to the end of the experiment		
Earliest Impact Date	From the moment the pipe is installed	Latest Impact date	End of the experiment

Risk Long Title: Development of a leak on one calibration pipe.										
Risk Description: A leak in a pipe would lead to liquid argon entering the pipe; this could happen either at the level of a solder point or at the level of a below/flange where two sections of the pipes are joint and not soldered.										
Detailed Risk Cause: A defect in the solder; a mistake when installing the flange.										
Detailed Risk Effect: Severe; the Ti vessel would need to be emptied and the pipe repaired, or not ?										
Describe possible Mitigation Plan(s): Make sure the pipes do not leak; design a set of tests to validate welding and installation of flanges. Orbital welding is a well known process and expertise exists in the collaboration.										
WBS Affected: <i>use the WBS name here. Risk Mgr may fill in the WBS number</i>										
<table border="1"> <thead> <tr> <th>Probability, as %</th> <th>Cost Impact, in currency and value</th> <th>Schedule Impact in working Days</th> <th>Technical Impact</th> <th>Safety/Environment Impact</th> </tr> </thead> <tbody> <tr> <td>% ?????</td> <td>Experimental time lost</td> <td>One year</td> <td>Severe</td> <td>?</td> </tr> </tbody> </table>	Probability, as %	Cost Impact, in currency and value	Schedule Impact in working Days	Technical Impact	Safety/Environment Impact	% ?????	Experimental time lost	One year	Severe	?
Probability, as %	Cost Impact, in currency and value	Schedule Impact in working Days	Technical Impact	Safety/Environment Impact						
% ?????	Experimental time lost	One year	Severe	?						

Figure 51: Guide tube system Risk3

Risk ID	<i>The Risk Manager assigns this</i>		
Submitter	Isabelle Wingerter-Seez	Risk Owner	Jelena Maricic, Pierre Barrillon
Date	2021.11.16	Risk Short Title	Contamination by distributed sources
Risk Time Frame	From day 1 to the end of the experiment		
Earliest Impact Date	From the first day a source is introduced in the pipe	Latest Impact date	End of the experiment

Risk Long Title: The detector is contaminated with decay daughters from the distributed sources.				
Risk Description: Increased background rates.				
Detailed Risk Cause: One material is activated which was not tested before.				
Detailed Risk Effect: Severe. Rate increase of diffused backgrounds				
Describe possible Mitigation Plan(s): Fully characterize the behavior of the distributed sources using test detectors prior to deployment.				
WBS Affected: <i>use the WBS name here. Risk Mgr may fill in the WBS number</i>				
Probability, as %	Cost Impact, in currency and value	Schedule Impact in working Days	Technical Impact	Safety/Environment Impact
% ?????	Experimental time lost	90 days	Severe	Minimal

Figure 52: Guide tube system Risk4

D RISKS

Risk ID	<i>The Risk Manager assigns this</i>	Risk Type	Threat
Submitter	Isabelle Wingerter-Seez, Jelena Maricic	Risk Owner	Jelena Maricic
Date	2021.11.23	Risk Short Title	Leak in the sealing of gamma source
Risk Time Frame	From day 1 to the end of the experiment		
Earliest Impact Date	From the first day a source is introduced in the pipe	Latest Impact date	End of the experiment

Risk Long Title: The gamma source is not sealed properly and develops a leak during operation, leaking the radioactive material on the surface of the pipes.

Risk Description: Increased background rates due to pipe contamination.

Detailed Risk Cause: Improper sealing of the source capsule may lead to source leaks.

Detailed Risk Effect: Severe. Rate increase of gamma background in the pipe that would also affect veto detector, and edge of the TPC volume.

Describe possible Mitigation Plan(s): Test the source encapsulation prior to insertion for leaks. Perform repeated pressure tests to confirm that there are no leaks. *This risk is more an operational risk than a construction risk. Though its prevention is integrated in the design of the system.*

Figure 53: Source Risk1

Risk ID	<i>The Risk Manager assigns this</i>	Risk Type	Threat
Submitter	Isabelle Wingerter-Seez, Jelena Maricic	Risk Owner	Jelena Maricic, Pierre Barrilon
Date	2021.11.23	Risk Short Title	Deployment motor system malfunction
Risk Time Frame	From day 1 to the end of the experiment		
Earliest Impact Date	From the first day deployment system is used	Latest Impact date	End of the experiment

Risk Long Title: Malfunction of the deployment motor, may leave the source stuck in the pipe for extended periods of time, disrupting physics data taking.

Risk Description: Loss of physics data due to source extraction delays.

Detailed Risk Cause: Motor malfunction due to mechanical problem.

Detailed Risk Effect: Moderate. It extends physics data taking beyond planned.

Describe possible Mitigation Plan(s): As part of the design, build the capability for manual turning of the crank and retrieving the source, even in the motor dies.

Figure 54: Source Risk2

D RISKS

Risk ID	<i>The Risk Manager assigns this</i>	Risk Type	Threat
Submitter	Isabelle Wingerter-Seez, Jelena Maricic	Risk Owner	Alexandre Chepurnov
Date	2021.11.23	Risk Short Title	DD neutron generator stuck
Risk Time Frame	From day 1 to the end of the experiment		
Earliest Impact Date	From the first day deployment system is used	Latest Impact date	End of the experiment

Risk Long Title: DD neutron generator may get stuck at pipe bends.
Risk Description: Loss of physics data due to source extraction delays. Potential loss of the calibration capability if the DD neutron generator cannot be retrieved.
Detailed Risk Cause: DD neutron generator is significantly larger than the radioactive sources and therefore may get stuck inside the calibration pipe, particularly around the bends.
Detailed Risk Effect: Moderate. Creates data taking delay, and may permanently jeopardize calibration campaigns if the DD neutron generator cannot be retrieved.
Describe possible Mitigation Plan(s): Build the mock-up DD n generator and run it around the bend mock-up in the laboratory testing. Increase the pipe diameter to reduce the risk. Coat the Dd n generator with Teflon to make it slippery and easier to slide.

Figure 55: Source Risk3

Risk ID	<i>The Risk Manager assigns this</i>	Risk Type	Threat
Submitter	Isabelle Wingerter-Seez	Risk Owner	Jelena Maricic, Pierre Barrillon
Date	2021.11.23	Risk Short Title	Contamination by distributed sources
Risk Time Frame	From day 1 to the end of the experiment		
Earliest Impact Date	From the first day a source is introduced in the pipe	Latest Impact date	End of the experiment

Risk Long Title: The detector is contaminated with decay daughters from the distributed sources.
Risk Description: Increased background rates.
Detailed Risk Cause: One material is activated which was not tested before.
Detailed Risk Effect: Severe. Rate increase of diffused backgrounds
Describe possible Mitigation Plan(s): Fully characterize the behavior of the distributed sources using test detectors prior to deployment. <i>This risk is more an operational risk than a construction risk. Though its prevention is integrated in the design of the system.</i>

Figure 56: Source Risk4

E Background results for ArDM stainless steel

Element	^{238}U Upper	^{238}U Middle	^{238}U Lower	^{232}Th	^{235}U	^{40}K	^{60}Co	^{137}Cs
Contamination (mBq/kg)	50	50	50	20	2.3	6.4	13	1.5
Photon producer ?	Yes	Yes	Yes	Yes	Yes	Yes	Yes	Yes
Neutron producer ?	Yes	Yes	Yes	Yes	Yes	No	No	No
Neutron yield (neutron/decay)	1.1×10^{-9}	4.8×10^{-7}	1.06×10^{-9}	1.8×10^{-6}	3.7×10^{-7}	No	No	No

Table 27: For Stainless steel, assuming ArDM-type stainless steel: contamination sources inside the pipes and their respective contamination levels (mBq/kg), background production and neutron yield.

Element	^{238}U Upper	^{238}U Middle	^{238}U Lower	^{232}Th	^{235}U
Contamination (mBq/kg)	50	50	50	20	2.3
Neutron yield (neutron/decay)	1.1×10^{-9}	4.8×10^{-7}	1.06×10^{-9}	1.8×10^{-6}	3.7×10^{-7}
Events/10years	2.1×10^{-7}	9.1×10^{-5}	2.1×10^{-7}	1.4×10^{-4}	3.2×10^{-6}

Table 28: NR background rates induced by the radioactive contamination of the Stainless Steel pipes, assuming ArDM-type stainless steel, after normalisation (which includes the neutron production rate of the three radioactive elements).

Element	^{238}U Upper	^{238}U Middle	^{238}U Lower	^{232}Th	^{235}U	^{40}K	^{60}Co	^{137}Cs
Contamination (mBq/kg)	50	50	50	20	2.3	6.4	13	1.5
Events/10years	< 110	< 110	< 110	< 44	< 5	< 14	< 28	< 3.3

Table 29: ER background rates induced by the radioactive contamination of the Stainless Steel pipes, assuming ArDM-type stainless steel, after normalisation.